Control of Oxidation−Reduction Potentials in Flavodoxin from *Clostridium beijerinckii*: The Role of Conformation Changes[†,‡]

Martha L. Ludwig,* Katherine A. Pattridge, Anita L. Metzger, and Melinda M. Dixon

Biophysics Research Division and Department of Biological Chemistry, University of Michigan, Ann Arbor, Michigan 48109-1055

Mesut Eren, Yucheng Feng, and Richard P. Swenson

Department of Biochemistry, The Ohio State University, Columbus, Ohio 43210

Received August 27, 1996; Revised Manuscript Received November 26, 1996[⊗]

ABSTRACT: X-ray analyses of wild-type and mutant flavodoxins from *Clostridium beijerinckii* show that the conformation of the peptide Gly57-Asp58, in a bend near the isoalloxazine ring of FMN, is correlated with the oxidation state of the FMN prosthetic group. The Gly-Asp peptide may adopt any of three conformations: *trans* O-up, in which the carbonyl oxygen of Gly57 (O57) points toward the flavin ring; *trans* O-down, in which O57 points away from the flavin; and *cis* O-down. Interconversions among these conformers that are linked to oxidation−reduction of the flavin can modulate the redox potentials of bound FMN. In the semiquinone and reduced forms of the protein, the Gly57-Asp58 peptide adopts the *trans* O-up conformation and accepts a hydrogen bond from the flavin N5H [Smith, W. W., Burnett, R. M., Darling, G. D., & Ludwig, M. L. (1977) *J. Mol. Biol. 117*, 195−225; Ludwig, M. L., & Luschinsky, C. L. (1992) in *Chemistry and Biochemistry of Flavoenzymes III* (Müller, F., Ed.) pp 427−466, CRC Press, Boca Raton, FL]. Analyses reported in this paper confirm that, in crystals of wild-type oxidized *C. beijerinckii* flavodoxin, the Gly57-Asp58 peptide adopts the O-down orientation and isomerizes to the *cis* conformation. This *cis* form is preferentially stabilized in the crystals by intermolecular hydrogen bonding to Asn137. Structures for the mutant Asn137Ala indicate that a mixture of all three conformers, mostly O-down, exists in oxidized *C. beijerinckii* flavodoxin in the absence of intermolecular hydrogen bonds. Redox potentials have been manipulated by substitutions that alter the conformational energies of the bend at ^{56}M-G-D-E. The mutation Asp58Pro was constructed to study a case where energies for *cis*−*trans* conversion would be different from that of wild type. Intermolecular interactions with Asn137 are precluded in the crystal, yet Gly57-Pro58 is *cis*, and O-down, when the flavin is oxidized. Reduction of the flavin induces rearrangement to the *trans* O-up conformation. Redox potential shifts reflect the altered energies associated with the peptide rearrangement; E(ox/sq) decreases by ∼60 mV (1.3 kcal/mol). Further, the results of mutation of Gly57 agree with predictions that a side chain at residue 57 should make addition of the first electron more difficult, by raising the energy of the O-up conformer that forms when the flavin is reduced to its semiquinone state. The ox/sq potentials in the mutants Gly57Ala, Gly57Asn, and Gly57Asp are all decreased by ∼60 mV (1.3 kcal/mol). Introduction of the β-branched threonine side chain at position 57 has much larger effects on the conformations and potentials. The Thr57-Asp58 peptide adopts a *trans* O-down conformation when the flavin is oxidized; upon reduction to the semiquinone, the 57-58 peptide rotates to a *trans* O-up conformation resembling that found in the wild-type protein. Changes in FMN−protein interactions and in conformational equilibria in G57T combine to decrease the redox potential for the ox/sq equilibrium by 180 mV (+4.0 kcal/mol) and to increase the sq/hq potential by 80 mV (−1.7 kcal/mol). A thermodynamic scheme is introduced as a framework for rationalizing the properties of wild-type flavodoxin and the effects of the mutations.

Flavodoxins are an important class of electron transfer proteins that utilizes flavin mononucleotide as a prosthetic group. They are conveniently small (M_r < 20 kDa) molecules in which to investigate how flavin−protein interactions regulate the oxidation−reduction properties of the bound cofactor. Distinguishing features of these proteins include the thermodynamic stabilization of the blue neutral flavosemiquinone species and the very low potentials of the semiquinone/hydroquinone (sq/hq)[1] couple (Ludwig & Luschinsky, 1992). Association of FMN with the protein often raises the oxidized/semiquinone (ox/sq) potentials and uniformly lowers the semiquinone/hydroquinone potentials, relative to those of free FMN, eliciting substantial potential shifts. The sq/hq potentials in flavodoxins (−400 mV or less) are the lowest exhibited by any flavoprotein. The separation of the two potentials may represent an important

[†] This work was supported by grants from the National Institutes of Health (GM16429 to M.L.L. and GM46390 to R.P.S.).

[‡] The following coordinates have been deposited with the Brookhaven Protein Data Bank [WT, ox, 5nll; WT, sq, 2fox; WT, hq, 5ull; N137A, ox (277 K), 2fdx; N137A, ox (140 K), 2fax; N137A, hq, 6nul; G57A, ox, 3nll; G57N, ox, 1fvx; D58P, ox, 4nul; D58P, hq, 1fln; G57D, ox, 4nll; G57D, hq, 1fla; G57T, ox, 1fld; G57T, sq, 5nul; G57T, hq (277 K), 2fvx; G57T, hq (140 K), 2flv].

[⊗] Abstract published in *Advance ACS Abstracts,* January 15, 1997.

[1] Abbreviations: ox, oxidized; sq, semiquinone; hq, hydroquinone; SA, simulated annealing; WT, wild type.

S0006-2960(96)02180-0 CCC: $14.00

functional feature of flavodoxins, since they appear to act as low-potential one-electron carriers in the cell (Mayhew & Ludwig, 1975; Mayhew & Tollin, 1992).

Changes in the energies of protein−flavin interactions, which can occur when the cofactor is reduced, contribute to the redox potential shifts that are observed in flavodoxins and other flavoproteins. Protein−FMN interactions have therefore been examined in many flavodoxins using both X-ray and NMR techniques. Structures have been determined for the flavodoxins from *Desulfovibrio vulgaris* (Watenpaugh et al., 1976; Watt et al., 1991), *Clostridium beijerinckii* (Smith et al., 1977), *Micrococcus elsdenii* (van Mierlo et al., 1990), *Anacystis nidulans* (Smith et al., 1983; Laudenbach et al., 1988), *Chondrus crispus* (Fukuyama et al., 1992), *Anabaena variabilis* 7120 (Stockman et al., 1990; Rao et al., 1992; Burkhart et al., 1995), *Escherichia coli* (Hoover et al., 1994), and *Desulfovibrio desulfuricans* (Caldeira et al., 1994). Structural comparisons of oxidized with semiquinone and/or hydroquinone forms are available for the flavodoxins from *C. beijerinckii* (Smith et al., 1977; Ludwig & Luschinsky, 1992), *D. vulgaris* (Watt et al., 1991), *M. elsdenii* (van Mierlo et al., 1990), and *A. nidulans* (Luschinsky et al., 1991).

Structural and functional studies have established that electrostatic interactions are a dominant factor affecting the sq/hq equilibrium in flavodoxins. The flavin hydroquinone in flavodoxins is not protonated at N1 (Franken et al., 1984), and embedding the anionic isoalloxazine in the negatively charged protein environment found in flavodoxins generates substantial repulsions (Ludwig et al., 1990; Zhou & Swenson, 1995). As a consequence, flavin mononucleotide bound to flavodoxins is much more difficult to convert to the fully reduced form than is free FMN. The two-electron midpoint potentials of flavodoxins are lower than those of free FMN by 60−180 mV (2.6−7.8 kcal/mol), and the sq/hq potentials decrease by more than 200 mV (>4.6 kcal/mol). Examination of the known structures and extensive studies of mutations and modifications in the flavodoxins from *D. vulgaris* (Swenson & Krey, 1994; Stockman et al., 1994; Zhou & Swenson, 1995, 1996) and *C. beijerinckii* (Ludwig et al., 1990) show that unfavorable electrostatic and aromatic stacking interactions (and perhaps inaccessibility to solvent) can play critical roles in the thermodynamics of formation of fully reduced flavodoxin. Mutations in *D. vulgaris* flavodoxin have demonstrated a strong correlation of the sq/hq potential with the number of negatively charged groups in the neighborhood of the flavin (Zhou & Swenson, 1995).

The ox/sq potentials for well-characterized flavodoxins vary over a wide range (Mayhew & Ludwig, 1975; Mayhew & Tollin, 1992). The structural features and interactions that control this potential have not been fully elucidated. Reduction of oxidized flavodoxin to the semiquinone involves addition of one electron and one proton, and the ox/sq potentials do not appear to be very sensitive to electrostatic interactions (Zhou & Swenson, 1995). The flavodoxin from *C. beijerinckii* displays an unusually high midpoint potential for the oxidized/semiquinone couple, which at −92 mV is approximately 150 mV more positive than that of FMN free in solution. This increase in potential is one of the largest found in the flavodoxin family and is the focus of the studies described in this paper. Initial X-ray analyses of *C. beijerinckii* flavodoxin indicated that reduction to the semiquinone is coupled to a reorientation ("flip") of the carbonyl group of the peptide bond at Gly57-Asp58 [Smith et al., 1977; Ludwig et al., 1991; reviewed in Ludwig and Luschinsky (1992)]. Conformation changes that are linked to reduction in this fashion can affect the potentials in two ways, first by altering flavin−protein contacts and thereby the energies for FMN binding and second by altering the stability of the polypeptide itself. Peptide flips associated with reduction also occur in bends or loops near the FMN in the flavodoxins from *A. nidulans* (Laudenbach et al., 1988; Luschinsky et al., 1991) and *D. vulgaris* (Watenpaugh et al., 1976; Watt et al., 1991). However, there is no simple correspondence between the occurrence of these backbone rearrangements and a high ox/sq potential, and the ways in which conformation changes affect the energetics of reduction may differ among flavodoxins. In this paper, we appraise the role of conformation changes in flavodoxin from *C. beijerinckii*, taking two approaches. The conformation of residues Gly57-Asp58 in oxidized flavodoxin has been examined in wild-type flavodoxins, and mutants with substitutions at positions 57 and 58 have been characterized and analyzed by X-ray crystallography.

The initial studies of oxidized *C. beijerinckii* flavodoxin did not definitively assign the conformation of the peptide Gly57-Asp58 (Ludwig et al., 1976; Smith *et al.*, 1977). Using data to a resolution of 1.7 Å, we have reexamined the conformations of this peptide in the oxidized species of wild-type *C. beijerinckii* flavodoxin. Crystallographic refinement of the structure, presented in detail here and summarized in a preliminary report (Ludwig et al., 1994), demonstrates that the 57-58 peptide adopts a *cis* conformation in crystals of wild-type flavodoxin. However, this conformation appears to be preferentially stabilized by intermolecular interactions with a neighboring Asn137 in the crystal. X-ray analyses of the mutant N137A, in which these intermolecular interactions at the 57-58 peptide are eliminated, reveal a mixture of what we term "up" and "down" conformers (Figure 1) in oxidized clostridial flavodoxin. We assume that this mixture corresponds to the distribution of states in dilute solution under conditions where the redox potentials have been measured.

To study the impact of conformation changes on redox potentials, we have evaluated the effects of introducing the simple side chain substituents, Ala, Asp, and Asn, at position 57. These mutations were selected because they were expected to affect the relative stabilities of the accessible Gly57-Asp58 conformations. Furthermore, Asn was an interesting substitution since it is found at the position equivalent to Gly in several other flavodoxins (Ludwig & Luschinsky, 1992). In the semiquinone and fully reduced oxidation states, Gly57 of clostridial flavodoxin adopts the O-up conformation (Figure 1). This conformation resembles the orientation found in type II′ turns and is rarely populated by residues other than glycine (Smith & Pease, 1980; Wilmot & Thornton, 1988). Any other residue at this position would significantly increase the conformational energy of the reduced states, making reduction to the semiquinone more difficult. As expected, a primary result of mutation of Gly57 to Ala, Asn, or Asp is a lower redox potential for the ox/sq couple.

The mutants D58P and G57T were also constructed in attempts to lock the conformation of the 57-58 peptide by introduction of rigid or sterically hindered side chains. Despite the steric restrictions introduced by the proline and

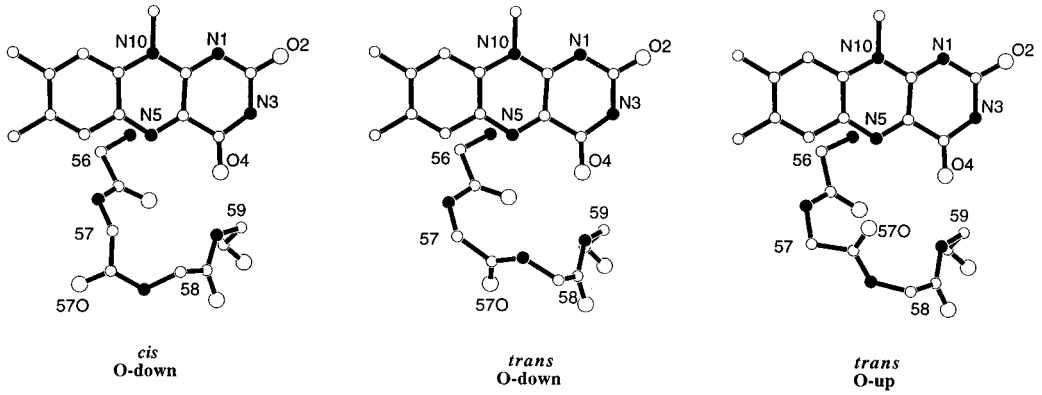

FIGURE 1: Conformations of the peptide backbone at residues 56−59 in *C. beijerinckii* flavodoxin. The position of O57 and the configuration of the peptide are the features that distinguish the three observed conformers. In the O-up form, the carbonyl oxygen of residue 57 is hydrogen-bonded to the flavin N5H. Side chains have been omitted to simplify the drawings. Nitrogen atoms are filled; C and O atoms are open, with larger radii assigned to the oxygens. Residues are numbered at the Cα atoms. The heteroatoms of the isoalloxazine ring are labeled, and the ribityl side chain has been omitted beyond C1′.

threonine side chains, each of these mutants still displays redox-linked rearrangements that bring O57 near to the flavin N5H in the semiquinone and reduced states. X-ray analyses of the mutant D58P establish that the Gly57-Pro58 peptide undergoes *cis*−*trans* isomerization when the crystalline protein is reduced. Substitution of threonine for Gly57 alters the distribution of conformations in the oxidized state and affects the redox-linked equilibrium between O-down and O-up conformations (Figure 1). In this mutant, changes in interactions between the flavin semiquinone and the apoprotein can also be detected. The effects of the G57T mutation combine to decrease the redox potential for the ox/sq equilibrium by 180 mV (+4.0 kcal/mol) and the potential for two-electron reduction by 50 mV (+2.3 kcal/mol). Taken together, the structures and properties of the mutant proteins demonstrate that conformational energies can modulate the ox/sq potential and confirm the importance of interactions between the O-up peptide and the flavin for stabilizing the semiquinone oxidation state.

MATERIALS AND METHODS

Materials. Oligonucleotides used for mutagenesis were synthesized on an Applied Biosystems Model 380B synthesizer by the Biochemical Instrument Center, a core biopolymer service facility of The Ohio State University, and purified by reverse phase high-performance liquid chromatography using standard protocols. The *E. coli* XL1-Blue cell line was from Stratagene. Restriction endonucleases and T4 DNA ligase were purchased from GIBCO BRL Life Technologies, Inc. The Sequenase DNA sequencing kit was obtained from United States Biochemical Corp. Isopropyl thiogalactoside was purchased from Boehringer Mannheim Corp. Phenosafranine dye was obtained from Allied Chemical Co. Hydroxyethyl viologen was synthesized as described previously and recrystallized from methanol (Kazarinova et al., 1967). Benzyl viologen was purchased from Serva Chemicals. All other redox indicator dyes were obtained from the Fluka Chemical Co. and were used without further purification. Safranine T was recrystallized from hot 95% ethanol before use. All other reagents are analytical grade.

Site-Directed Mutagenesis. Unless otherwise indicated, mutations were generated in the plasmid *pKK*Flasygen containing the previously constructed synthetic structural gene coding for the flavodoxin from *C. beijerinckii* (Eren & Swenson, 1989). This construction places the structural gene within the *Eco*RI and *Hin*dIII sites of the expression vector *pKK*223-3 (Pharmacia/LKG), immediately behind the inducible hybrid *tac* promoter (Amman et al., 1983) for heterologous expression in *E. coli.* The distribution of unique restriction sites throughout the coding region as part of the design provides for the efficient use of cassette mutagenesis.

Table 1: Oligonucleotide Sequences for Mutagenesis

mutation	mutagenic oligonucleotides[a]
G57A, G57D G57N, G57T	*Nco*I [GCT] *Xho*I 5' CATG[AAC]GATGAAGTTC3' ::: :::::::::: 3' [TGA]CTACTTCAAGAGCT5' [CGA]
D58P	*Nco*I *Ava*II *Xho*I 5' CATGGGT[CCG]GAAGTTC3' ::: ::: ::::::: 3' CCA[GGC]CTTCAAGAGCT5'
D58S	*Nco*I *Ban*II *Xho*I 5' CATGGGC[TCT]GAAGTTC3' ::: ::: ::::::: 3' CCG[AGA]CTTCAAGAGCT5'
N137A	5' AGATCGCG[GCC]ATCTAGTAG3'

[a] Mutations at positions 57 and 58 were introduced using the double-stranded casettes as shown. The N137A mutation was introduced using the single mutagenic oligonucleotide primer. The nucleotides in brackets are those which introduce the desired amino acid substitutions. For the G57 substitutions, 50% mixtures of each of the two nucleotides shown at each position were incorporated in each strand. The *Ava*II, created both by the codon substitution and by a "silent" mutation, and the *Ban*II restriction sites are introduced in each case for ease in screening transformants.

The codons for Gly57 and Asp58 fall between the *Nco*I and *Xho*I restriction sites which are separated by 11 base pairs (Eren & Swenson, 1989). Mutations at these sites were introduced using cassettes comprised of two complementary oligonucleotides spanning the two sites. The nucleotide sequence of each oligonucleotide was designed to contain the necessary redundancies at the relevant positions in the Gly57 codon to introduce the amino acid substitutions G57A, G57D, G57N, and G57T or, in two separate additional mutagenesis procedures, to introduce the amino acid substitutions D58P and D58S. The nucleotide sequences within each mutagenic cassette are summarized in Table 1. A mixture of the two oligonucleotides comprising each cassette

was phosphorylated and ligated to *Nco*I/*Xho*I-digested *pKK*Flasygen which had been dephosphorylated and purified from low-melting agarose using standard procedures (Maniatis et al., 1982). Competent *E. coli* XL1-Blue cells were transformed with a portion of the ligation mixture.

Plasmids from a representative sample of transformants were screened for mutants in the following way. The G57A and G57D mutants were initially identified by the inability of the restriction enzyme *Nco*I to linearize the plasmids due to the destruction of this recognition site by these mutations. The two mutants were distinguished from one another by the unique banding patterns generated by double-lane dideoxynucleotide sequencing using ddGTP and ddCTP. The G57T and G57N mutants were identified similarly using ddATP and ddCTP. In each of two separate mutagenesis experiments, transformants containing plasmids with the D58P or D58S mutation were initially identified by the unique restriction maps generated by the introduction during mutagenesis of the additional *Ava*II and *Ban*II restriction sites, respectively (see Table 1). All mutations and the integrity of the entire coding region were confirmed by the Sanger dideoxynucleotide sequencing procedure (Sanger et al., 1977) using the Sequenase protocol.

The N137A mutation was generated by standard oligonucleotide-directed mutagenesis using the Kunkel method for enriching mutant transformants (Kunkel et al., 1987). In addition to introducing the desired amino acid substitution, the mutagenic oligonucleotide sequence (Table 1) was also designed to eliminate a *Nru*I site for efficient screening. The single-stranded, uracil-containing template for mutagenesis was prepared by standard methods using the plasmid *p*BS(−)*tac*Flasygen. This latter construction was prepared by cloning the *Bam*HI/*Hin*dIII fragment from *pKK*Flasygen into the *p*Bluescript SK(−) phagemid (Stratagene), which in addition to the flavodoxin gene includes a 260 bp 5′-flanking sequence from the pKK223-3 plasmid containing the *tac* promoter. The N137A flavodoxin mutant was expressed directly in *E. coli* from this phagemid construction.

Expression and Purification of the Flavodoxin Mutants. Transformed *E. coli* XL-1 Blue cells were cultured for 15−24 h at 37 °C with agitation in NZY medium containing 100 mg/ml ampicillin. On some occasions, expression was induced by the addition of isopropyl thiogalactoside (IPTG) to a final concentration of 1 mM after cells had reached an optical density of 0.7−1.0 at 600 nm. Substantial expression was observed in the absence of IPTG induction, however (Eren & Swenson, 1989). Cells were harvested by centrifugation at 6000*g*, resuspended in 50 mM Tris-HCl at pH 7.3, and lysed by a single passage through a French press cell at 12000−15000 psi. The flavodoxin holoprotein was isolated from the supernatant by a modification of the method described by Mayhew and Massey (1969). The supernatant fraction was applied to a DEAE-cellulose column equilibrated in 50 mM Tris-HCl at pH 7.3 (determined at 25 °C) and washed with 50 mM Tris-HCl at pH 7.3 containing 150 mM NaCl. After the absorbance at 280 nm the wash solution returned to a value less than 0.1, the flavodoxin protein was eluted with the Tris buffer containing 225 mM NaCl. The fractions containing flavodoxin holoprotein were pooled, diluted with an equal volume of Tris buffer, and loaded on a second smaller column of DEAE-cellulose. The column was washed with 50 mM Tris-HCl at pH 7.3 containing 150 mM NaCl until the absorbance at 280 nm was less than 0.05, and the flavodoxin eluted with Tris buffer containing 200 mM NaCl. Fractions having a A_{274}:A_{457} ratio of *ca.* 4 were pooled and concentrated by ultrafiltration. The purity of each flavodoxin preparation was confirmed by SDS−polyacrylamide gel electrophoresis.

Ultraviolet/Visible Absorbance Spectroscopy. The near-ultraviolet/visible absorbance spectra of the purified flavodoxin proteins were recorded on either a Kontron UVIKON 810 dual-beam or a Hewlett-Packard 8452A photodiode array spectrophotometer. Extinction coefficients of the mutant flavodoxins in the fully oxidized state were determined as described by Mayhew and Massey (1969). An extinction coefficient of 12 500 M^{-1} cm^{-1} at 445 nm for the released FMN was used in the calculations (Whitby, 1953).

The absorbance properties of the semiquinone and fully reduced forms of each mutant flavodoxin were determined during anaerobic reduction in 50 mM sodium phosphate at pH 7.0 with sodium dithionite and/or reduction by NADPH in the presence of catalytic amounts of spinach ferredoxin−NADP reductase. With the exception of the G57T mutant, the extinction coefficient of the semiquinone at the λ_{max} in the 580 nm region was determined from the intercept of the extrapolation of the linear portions of plots of the 580 nm absorbance versus the volume of reductant.

Determination of Oxidation−Reduction Potentials. The midpoint potential of the ox/sq couple of each flavodoxin was determined spectrophotometrically at 25 °C by equilibration with standard redox indicator dyes in 60 mM sodium phosphate at pH 7.0 at various points during anaerobic titration with sodium dithionite. Protein and dye concentrations varied from 25 to 40 μM. Each sample, contained within a special sealable titration cuvette, was made anaerobic by repeated cycles of partial vacuum evacuation and flushing with prepurified argon which had been passed through an oxygen-eliminating catalyst trap (R&D Separations Oxygen Getter cartridge). The indicator dyes utilized in the determination of the midpoint potential of the ox/sq couple included indigo disulfonate ($E_{m,7} = -116$ mV), 2-hydroxy-1,4-naphthoquinone ($E_{m,7} = -145$ mV), anthraquinone 2,6-disulfonate ($E_{m,7} = -184$ mV), anthraquinone 2-sulfonate ($E_{m,7} = -225$ mV), phenosafranine ($E_{m,7} = -255$ mV), and/or safranine T ($E_{m,7} = -276$ mV). The reduction potential of the sq/hq couple was determined as above by equilibration with safranine T, benzyl viologen ($E_{m,7} = -359$ mV), and/or 2-hydroxyethyl viologen ($E_{m,7} = -408$ mV). Concentrations of the various oxidized and reduced species in equilibrium during the step-wise reduction were determined by multicomponent linear regression analysis of the near-ultraviolet/visible spectrum. Midpoint potentials were calculated using the Nernst equation or, in the case of the viologen dyes, from the evaluation of the equilibrium constant by methods described previously (Swenson & Krey, 1994; Zhou & Swenson, 1995).

Estimation of the pK of N5H in the Semiquinone Species. The p*K* for conversion of the blue neutral semiquinone to the red anionic form was estimated from spectral changes that occurred following pH jumps (Ludwig et al., 1990). Stock solutions of the G57T mutant flavodoxin (pH 6.02, 0.01 M potassium phosphate, OD of 0.6 at 454 nm) and of recombinant wild-type flavodoxin (pH 6.80, 0.01 M potassium phosphate, OD of 0.7 at 454 nm) were converted to the semiquinone forms by photoreduction (Massey & Hemmerich, 1978) in the presence of deazariboflavin (0.5 μM)

Table 2: X-ray Data for Wild-Type and Mutant Flavodoxins

crystal	method[a] (temp)	cell dimensions[b] (a=b, c, Å)	R_{sym} (%)	% complete	resolution (Å)	R-factor
WT, ox	MW (−10 °C)	61.48, 70.18	7.9	90.6	10−1.75	0.186
WT, sq[c]	Diff (4 °C)	61.63, 70.98		99.7	10−1.8	0.195
WT, hq	Diff (4 °C),	61.68, 71.05		87.1	10−1.8	0.182
N137A, ox[d]	MW (4 °C)	61.47, 70.76	6.5	98.2	10−1.65	0.190
N137A, ox	MW (140 K)	60.82, 69.61	5.25	99.3	10−1.8	0.175
N137A, hq	MW (140 K)	60.68, 69.54	6.32	97.8	10−1.8	0.179
G57A, ox	MW (4 °C)	61.48, 70.29	2.55	96.1	10−2.4	0.150
G57N, ox	MW (4 °C)	61.52, 70.77	6.01	99.4	10−1.9	0.176
D58P, ox	MW (4 °C)	61.51, 70.89	6.52	98.7	10−1.9	0.167
D58P, hq	MW (4 °C)	61.64, 71.01	5.19	97.3	10−1.9	0.169
G57D, ox	MW (4 °C)	61.47, 70.52	6.43	95.6	10−1.9	0.170
G57D, hq	MW (4 °C)	61.58, 71.35	5.08	99.5	10−1.9	0.183
G57T, ox	MW (4 °C)	61.53, 70.83	3.97	97.7	10−1.8	0.173
G57T, sq	MW (140 K)	60.88, 69.79	6.75	94.3	10−1.6	0.183
G57T, hq	MW (4 °C)	61.59, 71.08	5.28	96.4	10−1.8	0.174
G57T, hq	MW (140 K)	60.98, 70.16	6.82	97.6	10−1.8	0.180

[a] MW refers to multiwire area detector and Diff to diffractometer. [b] In WT flavodoxin and in some of the mutants, reduction is accompanied by changes in the unit cell dimensions. [c] Measurements from multiple crystals were scaled and combined. [d] Measurements for two crystals were scaled together.

and EDTA (5 mM). Protocatechuate dioxygenase and protocatechuate (0.1 mM) were added to scavenge oxygen (Bull & Ballou, 1988). The wild-type protein was converted in a stepwise series of irradiations to ∼100% semiquinone, but the maximum yield of semiquinone for the G57T mutant was 65% as expected from the measured potentials (see below).

In stopped-flow experiments, the photoreduced mutant and wild-type proteins were mixed with equal volumes of 0.1−0.2 M buffers: phosphate at pH 6.0 and 6.8 (controls), glycine at pH 9.8, phosphate at pH 11.5, and with 0.1 and/or 0.4 N KOH. Spectral changes were followed by rapid scanning of the absorbance between 350 and 700 nm, using a Hi-Tech Scientific diode array stopped-flow spectrophotometer.

Crystallization and Data Collection. For determination of structures of oxidized flavodoxins, crystals of recombinant wild-type (Eren & Swenson, 1989) and mutant flavodoxins were grown from solutions of the oxidized proteins at 4 °C, using the hanging drop technique to equilibrate protein−precipitant solutions against 2.5−2.8 M ammonium sulfate buffered with Tris or phosphate (pH 6.8). Two of the mutant proteins, D58P and N137A, did not crystallize readily but were induced to nucleate by microseeding with wild-type clostridial flavodoxin. The small hexagonal prisms that grew from these seeds were in turn used as macroseeds to develop (in one or two cycles) crystals large enough for data collection. The crystals of wild-type protein in the semiquinone state (Table 2) were grown in a nitrogen-filled glovebox by dialysis of semiquinone flavodoxin against ammonium sulfate (Ludwig et al., 1969; Smith et al., 1977).

Controlling reduction of crystals to form the intermediate semiquinone is not simple, and we therefore focused on characterization of the fully reduced forms of the mutant flavodoxins. Reaction of crystals with excess sodium dithionite (20−40 mM in buffered 2.6−2.8 M ammonium sulfate) under anaerobic conditions reduces the bound FMN to the hydroquinone form. Individual crystals suspended in a holding solution were first transferred to melting point capillaries and then introduced into an argon-filled glovebox (Plaslab, Lansing, MI); dithionite solutions, prepared using anaerobic buffered ammonium sulfate as described (Correll, 1992), were added to the capillaries. In all cases, the extent of reduction was estimated from the color of the crystals, which are pale yellow when completely reduced but are very dark wine-red in color (Eaton et al., 1975) at maximum concentrations of semiquinone. Except for the mutant G57T, conversion to the hydroquinone appeared to be complete when the pH was maintained at 8.0−8.5, where dithionite is a better reductant than at pH 7 (Mayhew, 1977). The rosy color of crystals of the G57T mutant, treated with excess dithionite at pH values of 8.0−8.5, suggested that they were incompletely reduced. The difficulty in reduction of crystals of the G57T mutant may arise from the low potential for addition of the first electron, which is calculated to be −360 mV at pH 8.5. In the special case of the G57T mutant, we also wanted to determine the structure of the semiquinone form. Because the G57T mutation results in potentials for the ox/sq and sq/hq equilibria that are separated by only 50 mV at pH 7 (Table 3), conversion to the semiquinone is necessarily incomplete at pH 7 and above. The most favorable pH for generation of the semiquinone form of this mutant is near 6.0, where the maximum semiquinone concentration in solutions should be about 65%. At pH 5.75−6.0 in the presence of limited concentrations of dithionite, crystals of the G57T mutant turn dark red-purple, and these conditions were used to prepare a crystal for flash-freezing.

Table 3: Oxidation−Reduction Midpoint Potentials for *C. beijerinckii* Flavodoxin Mutants[a]

flavodoxin	$E_{ox/sq}$	$E_{sq/hq}$	$E_{ox/hq}$
wild type	−92 (2.12)	−399 (9.20)	−245 (11.32)
G57A	−143 (3.30)	−373 (8.60)	−258 (11.90)
G57D	−140 (3.23)	−378 (8.72)	−259 (11.95)
G57N	−162 (3.76)	−372 (8.58)	−267 (12.31)
G57T	−270 (6.23)	−320 (7.38)	−295 (13.61)
D58S	−89 (2.05)	−381 (8.79)	−236 (10.89)
D58P	−155 (3.57)	−360 (8.30)	−257 (11.87)
FMN[b]	−238 (5.49)	−172 (3.97)	−205 (9.46)

[a] Midpoint potentials are reported in millivolts versus the standard hydrogen electrode at pH 7.0 and 25 °C. Corresponding ΔG values in kilocalories per mole follow in parentheses. The error in these determinations is estimated to be ±5 mV. $E_{ox/hq}$ is calculated from the individual one-electron potentials. [b] Values for FMN in solution at pH 7 are taken from Draper and Ingraham (1968). Anderson (1983) determined values of −314 and −124 mV for $E_{ox/sq}$ and $E_{sq/red}$, respectively.

Data collection methods, resolution, and other indices of the quality of the X-ray measurements are summarized in Table 2. X-ray data from crystals of mutants and oxidized wild-type flavodoxin were collected using a multiwire area detector (Area Detector Systems); each data set was obtained from a single crystal, unless otherwise noted in Table 2. For data collection at 4 °C, reduced crystals were transferred to X-ray capillaries in the glovebox (Correll, 1992). For the experiments in which crystals were flash-frozen in a cold nitrogen stream, 15% glycerol (v/v) was included in holding (and reducing) solutions and crystals were transferred from reducing solutions to the cold stream immediately after removal from the glovebox. The data for wild-type reduced flavodoxin were collected on a diffractometer at 4 °C using a flow cell to allow continuous flushing with buffered ammonium sulfate and 100 mM dithionite.

Crystal Structures and Refinements. Earlier descriptions of the structures of wild-type clostridial flavodoxin were based on results from two different refinement strategies, group least squares (Hoard & Nordman, 1979; Smith et al., 1977) and, later, restrained refinement in PROLSQ (Hendrickson, 1985; Ludwig & Luschinsky, 1992). For comparison of wild type with mutant structures, we have now refined all of the forms of clostridial flavodoxin listed in Table 2, using a uniform protocol in X-PLOR (Brünger, 1992; Brünger, et al. 1990). Refinement started with the models from PROLSQ refinement (Ludwig & Luschinsky, 1992). Our protocols commenced with rigid body refinement in the cases where cell dimensions had changed significantly. In standard rounds, overall temperature factor and positional refinement preceded simulated annealing from 2000 K. Annealing was followed by positional refinement and by overall and individual temperature factor refinements. Solvents and alternate conformations (see below) were then subjected to occupancy and temperature factor adjustment. Force field parameters for the protein were from Engh and Huber (1991); parameters for the flavin were modified from those used by Correll (1992), charges for the oxidized FMN calculated by K. Osapay (personal communication) were applied for all oxidized states and in the initial refinements of the semiquinone and reduced states. In the final rounds of refinement of semiquinone and reduced structures, the charges on isoalloxazine atoms were set to 0.0. Difference and electron density maps were inspected during the refinements and the models adjusted as necessary using the graphics program TOM (Cambillau & Horjales, 1987). A bulk solvent correction (Brünger, 1992) was included in all cases. Solvent molecules were added to the models if they appeared as peaks greater than 3σ in difference maps and made acceptable hydrogen bonds with protein or other solvents; they were removed if, after *B*-factor and occupancy refinement, their scattering contribution at 2.0 Å fell below 20−30% of that of an oxygen atom at rest at full occupancy. The number of waters associated with the asymmetric unit at the conclusion of refinement ranged from 98 to 115 for models based on data collected at 4 °C and from 161 to 186 for models based on data collected at 140 K.

Difference maps suggested the presence of alternate conformations of the 57-58 peptide in the oxidized form of the N137A mutant and in the semiquinone and reduced forms of the G57T mutant. In the case of the N137A mutant, the model includes all three conformers: *trans* O-up, *trans* O-down, and *cis* O-down (Figure 1). The alternate conformers were first refined separately by standard protocols, and in preparation for occupancy refinement, residues 56−59 were then omitted from an additional round of refinement in order to remove model bias. Finally, the refined alternate conformers were included in the model for cycles of occupancy and *B*-factor refinement. The models for reduced and semiquinone forms of G57T include only the *trans* O-up and *trans* O-down species. The alternate models were refined together in iterative cycles of SA, positional, and occupancy refinement. Because of the correlation of temperature factors with occupancy and the overlap of model atoms in several conformers (see Figure 1), the relative occupancies cannot be determined accurately, particularly in the N137A model that includes three alternative conformations.

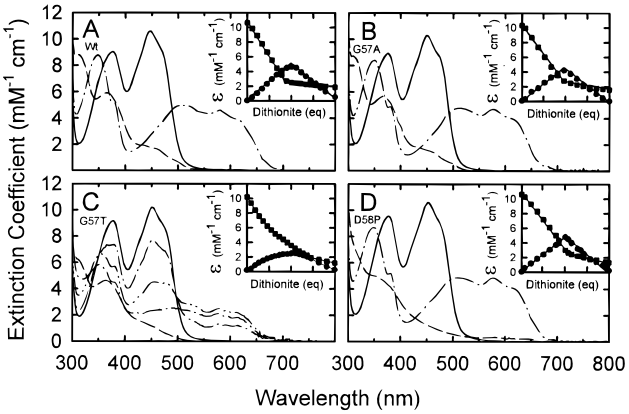

FIGURE 2: Near-ultraviolet/visible absorbance spectra of the recombinant wild-type *C. beijerinckii* flavodoxin (A) and the G57A (B), G57T (C), and D58P (D) mutant flavodoxins during reduction with sodium dithionite under anaerobic conditions. In each panel, the spectrum for the fully oxidized flavodoxin is denoted by the solid line, the partially reduced or semiquinone species by the dot-dashed line(s), and the fully reduced state by the dashed line. Flavodoxin (*ca.* 30 μM) in 50 mM phosphate buffer at pH 7.0 was titrated under argon in a sealed titration cuvette at 25 °C. For ease in comparisons, spectra of the fully formed semiquinone species of the wild type and G57A and D58P mutants were generated by the subtraction of the contribution of the small amount of oxidized and reduced species present near the midpoint of the titration and rescaled to 100%. The partially reduced spectra for the G57T mutant (C) have not been normalized and represent the actual level of semiquinone present at each point in the titration. The hydroquinone spectrum in each case was corrected for the presence of a small amount of semiquinone remaining at the end of the titration. The inset in each panel represents the changes in absorbance at the λ_{max} in the 450 nm (squares) and 575 nm (circles) regions as a function of the one-electron equivalents of sodium dithionite added to the titration mixture. In some cases, the small amount of dithionite that was consumed as the consequence of residual oxygen remaining in the flavodoxin solution has been subtracted.

RESULTS

Characterization of Mutant Flavodoxins

Spectral Properties. All the mutant flavodoxins described in this work were purified as the holoproteins. In the oxidized state, the UV/visible spectral characteristics of these mutants were similar to those of the wild-type protein. Relative to that of the wild-type protein, a small red shift of 5−7 nm in the absorbance maximum near 450 nm was noted in the oxidized forms of the Gly57 and D58P mutants (see Figure 2). The D58S mutant has spectral characteristics essentially identical to those of wild type. In all cases, the

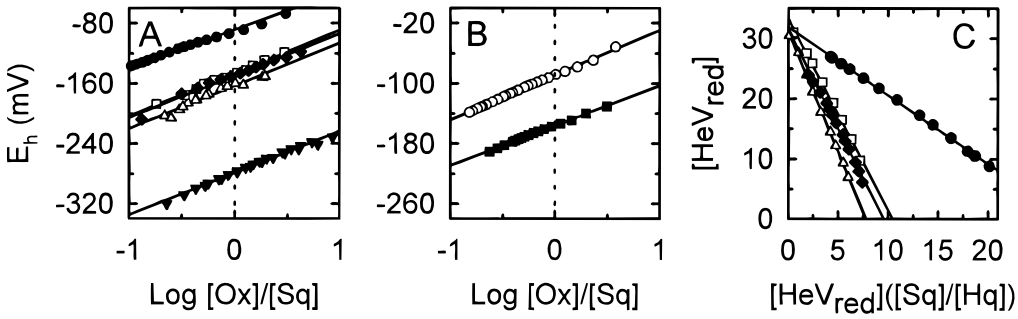

FIGURE 3: Determination of the midpoint potential for the ox/sq couple of wild type and the Gly57 mutants (A) and D58 mutants (B) and for the sq/hq couple of representative mutants (C). In each case, the one-electron reduction potentials were determined during the reductive titration with either sodium dithionite or NADPH in the presence of catalytic amounts of spinach ferredoxin−NADPH reductase. Titrations were performed at 25 °C under strict anaerobic conditions by equilibrium of the flavodoxin (*ca.* 30 μM), in 50 mM NaP_i at pH 7.0 with approximately 30 μM redox indicator dye as denoted in Materials and Methods. Titration data for the ox/sq couple are plotted according to the linear form of the Nernst equation. System potentials (E_h) were obtained from the ratio of the concentrations of the oxidized and reduced forms of the indicator dye. One-electron reduction potentials for the sq/hq couple are calculated from the equilibration between the flavodoxins and 2-hydroxyethyl viologen (HeV) during the reductive titration (C) as described in Materials and Methods. Symbols in each panel represent the data obtained for each flavodoxin as follows: recombinant wild type (closed circles), G57A (closed diamonds), G57D (open squares), G57N (open triangles), G57T (closed triangles), D58S (open circles), and D58P (closed squares).

position of the absorbance maximum in the near-ultraviolet region was at 377 nm, the same as in wild type. The extinction coefficients at the absorbance maximum in the 450 nm region were all quite similar, with an average value of 10 200 M^{-1} cm^{-1} compared with the published values of 10 400 M^{-1} cm^{-1} for the wild-type protein (Mayhew, 1971) and 10 600 M^{-1} cm^{-1} for the recombinant protein (Eren & Swenson, 1989).

Under anaerobic conditions, reduction of the G57A, G57D, G57N, D58P, and D58S mutants, as with the wild-type protein, proceeds in two separate one-electron steps with the nearly stoichiometric accumulation of the blue neutral semiquinone at the midpoint of the titration (spectra for representative mutants are shown in Figure 2). Each of the reductive steps was well-separated, with isosbestic points maintained throughout at least 95% of each part of the titration. The absorbance changes in the 450 nm region and at 575 nm were proportional to the amount of reductant added for each part of the reductive titration (Figure 2 insets). In contrast, all three oxidation states were present in significant amounts throughout most of the reductive titration of the G57T mutant. At pH 7.0, the flavin semiquinone accumulated to a maximal level of about 52% of the total concentration of this mutant flavodoxin (Figure 2C).

The absorbance spectra of the semiquinone forms of the mutant flavodoxins were very similar to those of wild type (see Figure 2), displaying absorbance maxima at 350 ± 2, 510 ± 4, and 576 ± 2 nm and an extinction coefficient at 576 nm of 4700 ± 100 M^{-1} cm^{-1}. A spectrum for the G57T semiquinone could not be obtained directly because of the presence of the other oxidation states throughout the titration; however, representative spectra for the semiquinone, determined by deconvoluting spectra observed throughout the titration, appear to be very similar to those of the other mutants.

Oxidation−Reduction Potentials. The one-electron reduction potentials for each flavin couple were determined at pH 7 and 25 °C for each mutant by equilibration with appropriate redox indicator dyes having established $E_{m,7}$ values (Clark, 1972). The experimental data conform well with the Nernst equation, generating slopes of 59 ± 6 mV, consistent with one-electron equilibria at 25 °C (Figure 3, panels A and B). The midpoint potentials obtained for the ox/sq couple of the four Gly57 mutants are more negative than that of the wild-type protein (Table 3). The potentials of the G57A, G57D, and G57N mutants were quite similar to one another, ranging from −140 to −162 mV. The G57T mutant, however, displays the much lower midpoint potential of −270 mV. This value is significantly more negative than that for unbound FMN (−238 mV; Draper & Ingraham, 1968). The ox/sq midpoint potential for the D58P mutant is more negative than that for wild type by 63 mV, whereas the D58S mutant has an ox/sq potential very similar to that of the wild-type flavodoxin. The D58S substitution mimics the structure of the highly homologous flavodoxin from *Megasphera elsdenii* and was chosen as a conservative control for the D58P experiment, to evaluate the effects of eliminating the charged Asp58 side chain.

In every mutant, the midpoint potential for the sq/hq couple was more positive than that of wild type (Figure 3C, Table 3). The values for the G57A, G57D, and G57N mutants are comparable, all about 25 mV higher than that for the wild-type protein. Again, the G57T mutant displayed the most aberrant potential, some 80 mV less negative than that of wild type. The midpoint potential values obtained for G57T by equilibrium with the indicator dye(s) are compatible with the extent of semiquinone accumulation observed during the reductive titrations under anaerobic conditions. The difference in the midpoint potentials of the ox/sq (E_2) and sq/hq (E_1) couples for the G57T mutant is 50 mV and can be used to calculate the formation constant, K_f, of the semiquinone using the relationship

$$E_2 - E_1 = \frac{RT}{nF} \ln K_f$$

The calculated K_f value of approximately 7 predicts that the maximum level of semiquinone formed during the titration should be about 55% of the total flavodoxin concentration, a level that agrees very well with that observed during the reductive titrations (Figure 2C). The nearly stoichiometric accumulation of semiquinone observed for the other mutants is consistent with the large K_f values calculated from the large differences in the midpoint potentials of the two redox couples in these proteins.

In the D58P mutant, the sq/hq potential was shifted from −399 mV to a more positive value of −360 mV. This

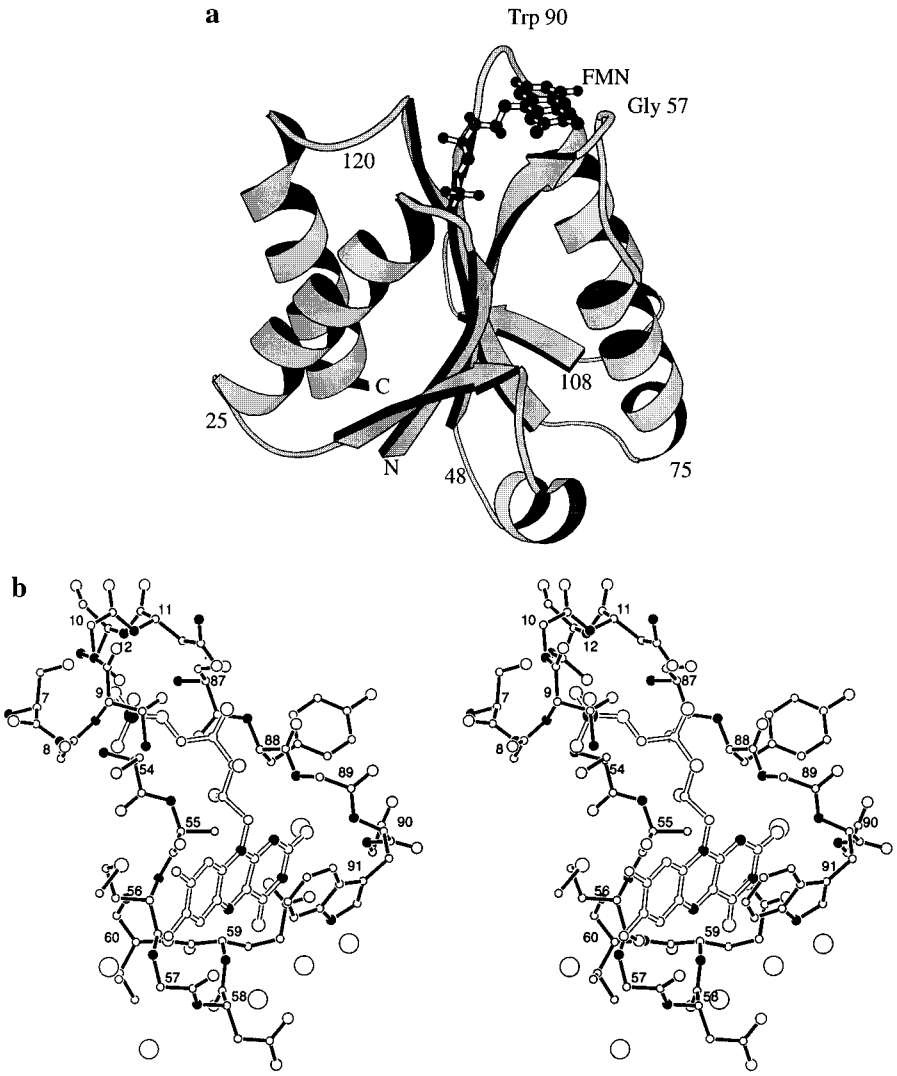

FIGURE 4: (a) Drawing (Kraulis, 1991) of flavodoxin from *C. beijerinckii*, showing the α/β-fold, the location of bound FMN, and the positions of Gly57 and Trp90 in loops that contact the isoalloxazine ring. (b) Stereodrawing depicting the FMN binding site of reduced *C. beijerinckii* flavodoxin. The prosthetic group is drawn with open bonds; solvents are drawn with large radii. The three regions of the protein that constitute the FMN binding site are shown in detail. The sequence ^{7}Ser-Gly-Thr-Gly-Asn-Thr binds the phosphate group; sequences ^{54}Ser-Ala-Met-Gly-Asp-Glu-Val and ^{87}Ser-Tyr-Gly-Trp-Gly interact with the flavin ring and ribityl side chain. Nitrogens are filled; C and O atoms are open, with larger radii assigned to the oxygens.

mutation alters the side chain charge as well as the energies for conformational transitions. The effect of eliminating charge interactions contributed by Asp58 can be estimated from the midpoint potential for the D58S mutant, which is −381 mV. It has been shown in other cases that the elimination or neutralization of acidic residues near the FMN cofactor can significantly increase the midpoint potential of the sq/hq couple (Ludwig & Luschinsky, 1992; Zhou & Swenson, 1995). However, no significant difference is observed between the sq/hq potentials of the mutants G57D and G57N. These side chains are exposed to solvent and are farther from the flavin N1 region than Asp58.

pK Measurements. The p*K* of N5H in the semiquinone form of the G57T mutant is reduced significantly, relative to that of wild type. Spectra recorded 3 ms after mixing the G57T mutant with pH 11.5 buffer (final pH of 11.3) displayed changes corresponding to partial conversion of the blue neutral to the red anionic semiquinone. Subsequent spectral transients in the time range of 8−128 ms corresponded to second-order disproportionation of the semiquinone species to a mixture of oxidized and reduced forms. From the changes in absorbance at 580 nm (λ_{max} for the neutral semiquinone), recorded at 3 ms, the N5H p*K* is estimated to be about 11.3. In agreement with this estimate, the spectrum immediately after jumping the pH to 12.5 showed almost no absorbance at 580 nm and had the characteristics of the red semiquinone, mixed with oxidized and reduced species. Control experiments with wild-type flavodoxin showed no evidence of formation of the red anionic form, even at a final estimated pH of 13.2, and confirm earlier studies indicating that the p*K* of N5H in the wild-type semiquinone is greater than 13.5 (Ludwig et al., 1990). After longer times at the highest pH values, the wild-type protein appeared to undergo both loss of flavin and disproportionation to form an equimolar mixture of oxidized and reduced free flavins.

Crystal Structures of Wild-Type and Mutant Flavodoxins

A drawing of flavodoxin from *C. beijerinckii*, in Figure 4a, shows the α/β-fold and the regions that constitute the FMN binding site. Assignments of the elements of secondary structure in wild-type oxidized flavodoxin, based on the

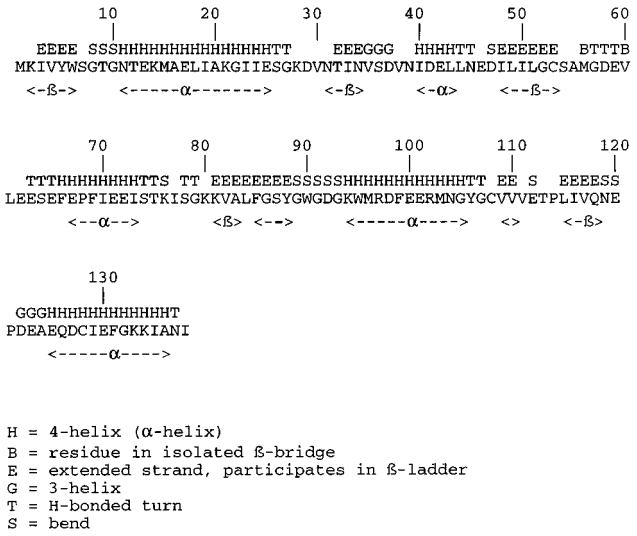

FIGURE 5: Secondary structures in flavodoxin from *C. beijerinckii*, as determined by the algorithm of Kabsch and Sander (1983). Their nomenclature is given below the sequence. Residues 40−43 form a turn of α-helix which was not designated as a helix in the initial descriptions of the structure (Burnett et al., 1974; Smith et al., 1977).

refinements reported here, are given in Figure 5. The FMN-binding determinants reside on three polypeptide segments (Figure 4b); each includes some unusual conformations, which are probably induced by interactions with the prosthetic group. The loop from Ser7 to Asn12 that binds FMN phosphate via NH···O hydrogen bonds has a characteristic shape that is highly conserved among flavodoxins (Ludwig & Luschinsky, 1992). Features of the other sequences, which interact with the flavin ring, vary among species in the flavodoxin family. In *C. beijerinckii* flavodoxin, the apolar side chains of Met56 and Trp90 contact the *re* and *si* faces of the flavin ring, respectively, while polar interactions between the isoalloxazine and apoflavodoxin are predominantly made by main chain atoms of the protein. Backbone NH groups in the sequence 88−91 interact with N1 and O2 at the pyrimidine end of the isoalloxazine ring, and these four successive residues form a bend with all the carbonyl oxygens on the same side of the polypeptide chain [cf. Reid and Thornton (1989)]. The turn formed by Met56-Glu59 contacts the N5 edge of the flavin ring; the only side chain in clostridial flavodoxin to form hydrogen bonds to the flavin ring is Glu59. The analyses reported here concentrate on the roles of this turn, or bend, in controlling redox equilibria. In the first of the following sections, backbone conformations and rearrangements that accompany reduction are described. The second section examines flavin−protein interactions and solvent interactions and considers how these vary with oxidation state and with the introduction of mutations at positions 57 and 58.

Conformations of Residues 56−59 in Wild-Type and Mutant Clostridial Flavodoxins

Oxidized Wild-type Flavodoxin and the Oxidized N137A Mutant. Although rearrangement of the polypeptide backbone at Gly57-Asp58, associated with reduction to the semiquinone, was established in early studies by Ludwig et al. (1976) and by Smith et al. (1977), the conformation in the oxidized form was not determined unambiguously. Initially, the structural change was interpreted as a transition from a distorted type II turn in oxidized flavodoxin to a type II′ turn in the semiquinone form. However, modeling of the oxidized conformer did not fully account for the electron density (Smith et al., 1977; Ludwig et al., 1976). Smith (1977) suggested that the 57-58 peptide bond might in fact be *cis* in oxidized flavodoxin, although no *cis* peptides had been observed with the sequence Gly-Asp. Restrained refinement (Hendrickson, 1985) and omit maps subsequently indicated that the peptide is *cis* in crystals of oxidized clostridial flavodoxin (Ludwig & Luschinsky, 1992).

To confirm the presence of the *cis* peptide, diffraction data for oxidized wild-type flavodoxin have been remeasured to 1.7 Å resolution at −10 °C (Table 2) and models have been refined as described in Materials and Methods. The starting models either incorporated a *cis* or a *trans* peptide bond joining residues Gly57 and Asp58 or omitted residues 56−59 altogether (Figure 6a). Maps with coefficients of $(2|F_o| - |Fc|) \exp(i\alpha_c)$ or $(|F_o| - |F_c|) \exp(i\alpha_c)$ were examined after full rounds of refinement that included simulated annealing (Brünger et al., 1990). The density in the omit maps and the absence of significant difference densities from maps computed after refinement of the *cis* conformer confirm that the *cis* bond assignment is correct. An additional verification of this assignment is shown in Figure 6a, which displays the alternate conformations in an omit map computed after refinement of the incorrect (*trans*) model.

As can be seen in Figure 6a, interactions with the symmetry-related Asn137 may preferentially stabilize the *cis* conformation in the crystal. The side chain of the Asn137 neighbor is able to make two hydrogen bonds to the backbone of the *cis* peptide, one to the carbonyl oxygen of Gly57 and the other to the NH of Asp58. However if the peptide is *trans*, only one hydrogen bond is possible since the intermolecular NH58 hydrogen bond cannot form. Construction of the mutant N137A and structure analysis of the expressed protein have allowed us to examine the effects of the interactions with Asn137 on the conformation of the 57-58 peptide. With data measured to 1.65 Å at 4 °C, maps of the oxidized N137A mutant were computed after refinement of each of the models: *cis* O-down, *trans* O-down, or *trans* O-up (see Figures 1 and 7a). In each case, difference densities suggested the presence of alternate conformers, implying that the crystal structure represents an equilibrium mixture of O-up and O-down conformers. To determine whether intensities measured at low temperature might clarify the interpretations, we collected data from a crystal of the oxidized protein at 140 K after flash-freezing. Difference maps again indicated the presence of a mixture of species. The higher-resolution 4 °C data were employed in further calculations to estimate the contributions of each conformer (See Materials and Methods). Inclusion of *trans* O-up and *trans* O-down conformers, omitting contributions from the *cis* O-down species, led to difference maps that suggested significant contributions from the *cis* form. Occupancy refinements including all three conformers yielded fractions that depended somewhat on the choices of temperature factors and on the occupancies assigned at the start of group refinement. The contribution of *trans* O-up is estimated to be about 30% and of *cis* O-down and *trans* O-down forms approximately 50 and 20%, respectively.

It is thus evident from the structural analysis of the N137A mutant that intermolecular hydrogen bonding between Asn137 and the 57-58 peptide has influenced the distribution of conformations in crystals of oxidized wild-type clostridial

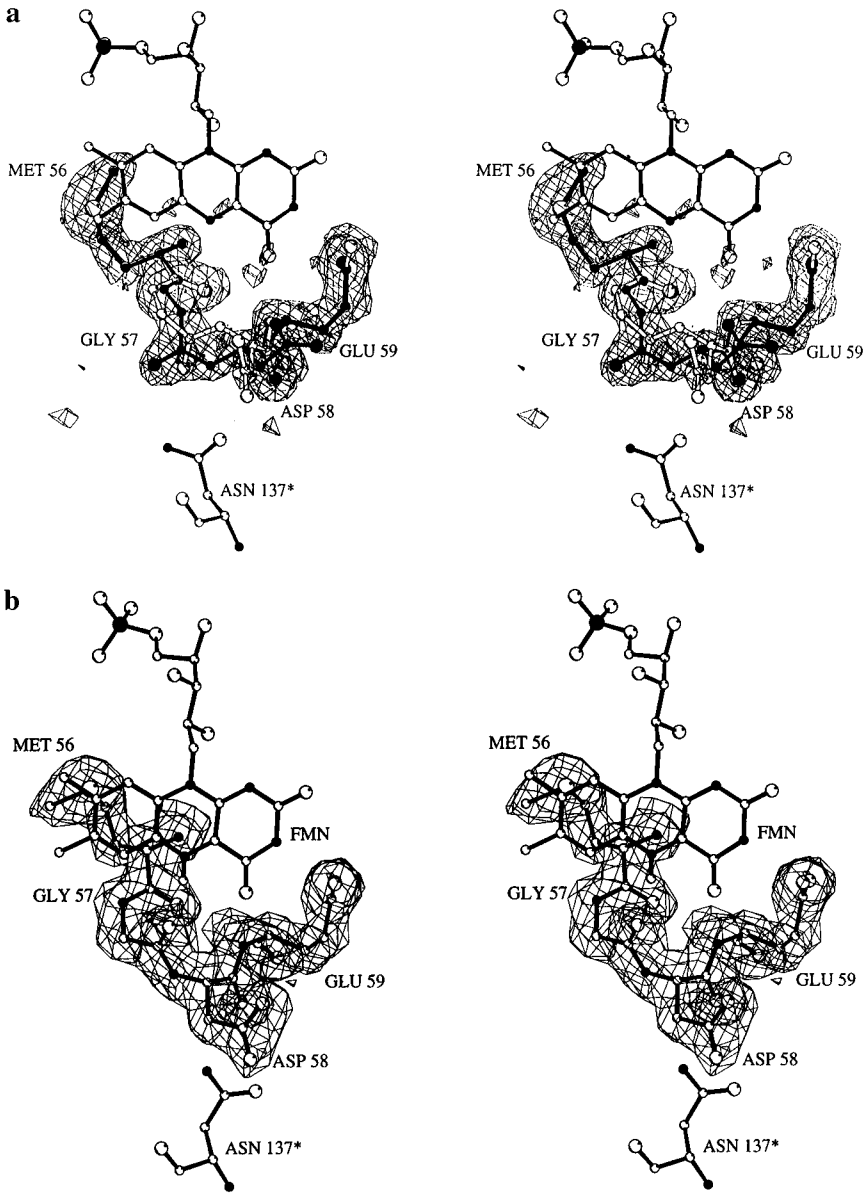

FIGURE 6: (a) Assignment of the conformation of residues 56−59 in oxidized wild-type flavodoxin. Refined models of *cis* (filled bonds) and *trans* (open bonds) conformers of the peptide Gly57-Asp58 are compared with the density in a map computed with amplitudes ($|F_o| - |F_c|$). $|F_c|$ and phases were from a refined *trans* model from which the contributions of residues 56−59 had been substracted. Hydrogen bonds between Gly and Asp and the Asn137* neighbor stabilize the *cis* peptide. Distances are as follows: O57−ND2 137*, 3.30 Å; and N58−OD1 137*, 2.88 Å. (b) Conformation of residues 56−59 in the semiquinone form of wild-type clostridial flavodoxin. Nitrogens are filled; C and O atoms are open, with larger radii assigned to the oxygens. The electron density is from a $2|F_o| - |F_c|$ map of the semiquinone form computed after refinement. The only contours shown are those corresponding to the atoms of residues 56−59.

flavodoxin. The structures found in the N137A mutant are likely to represent the situation that prevails in solution. This presumption implies the presence of some of the unusual *cis* conformer in solutions of oxidized wild-type *C. beijerinckii* flavodoxin.

Semiquinone and Reduced Forms of Wild-Type Flavodoxin and of the Mutant N137A. Structures have previously been described for the wild-type semiquinone (Smith et al., 1977) and for wild-type fully reduced species (Ludwig & Luschinsky, 1992). The earlier models were further refined against the data sets listed in Table 2 using X-PLOR. In both semiquinone and reduced wild-type flavodoxins, the Gly57-Asp58 peptide is clearly *trans* with O57 up in a position to accept a hydrogen bond from N5H (Figure 6b). There is no evidence for a mixture of conformations; at the conclusion of the X-PLOR refinements reported here, $|F_o| - |F_c|$ maps in the vicinity of the Gly-Asp peptide of semiquinone and reduced wild-type flavodoxins are featureless above 3σ. In wild-type flavodoxin, the peptide flip accompanying reduction breaks the hydrogen bonds with the neighboring Asn137, and the molecular packing and cell dimensions are altered (Smith et al., 1977).

A mixture of conformers at Gly57-Asp58 is found in the structure of the mutant N137A when the flavin is oxidized (see above), but reduction significantly alters the conformational equilibria. When crystals of the N137A mutant are reduced and then frozen at 140 K for collection of diffraction data, the 57-58 peptide adopts the *trans* O-up conformation that is also uniquely observed in crystals of the semiquinone and reduced wild-type proteins (Figure 6b). Electron density for the reduced N137A mutant is displayed in Figure 7b, and the observed conformation is compared with wild type in Table 4. We conclude that, while about 70% of the population of the oxidized mutant N137A molecules exists

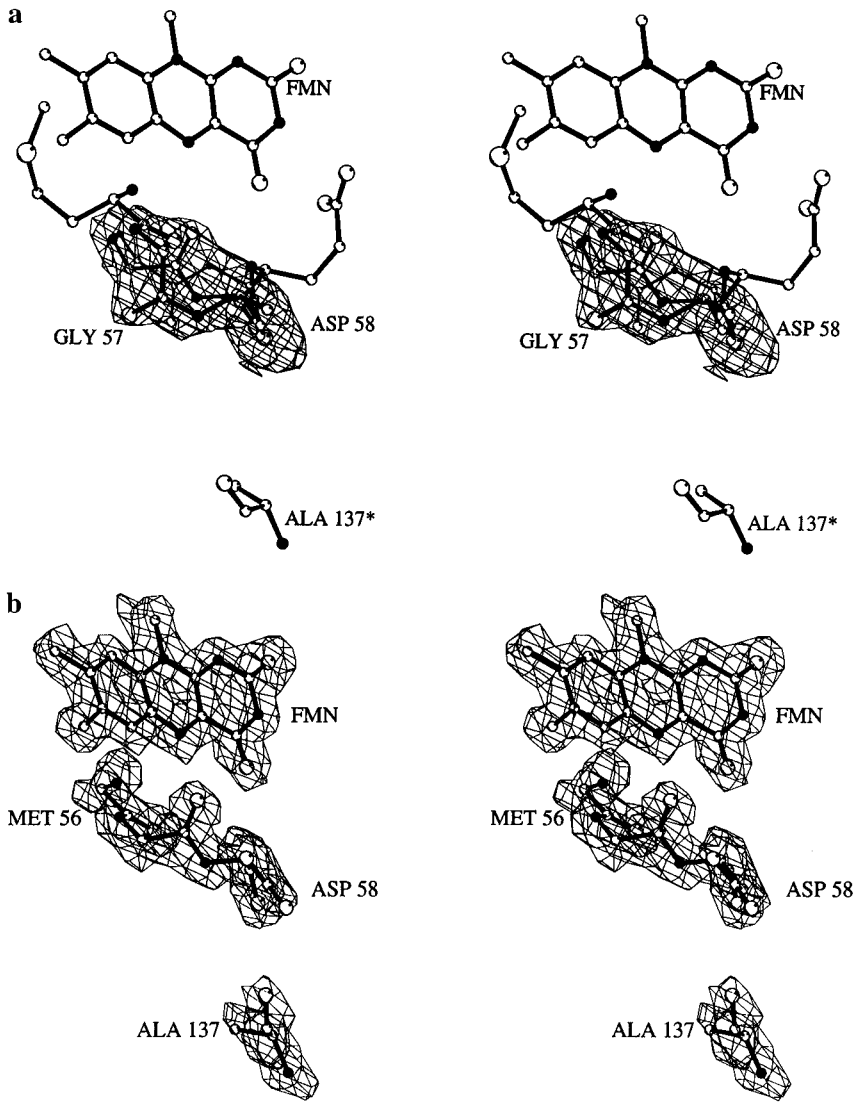

FIGURE 7: Drawings of the Gly57-Asp58 region of the structure of the mutant flavodoxin, N137A. (a) Electron densities from a $2|F_o| - |F_c|$ map computed after omit (56−59) refinement of the X-ray data measured at 4 °C from crystals of the oxidized N137A mutant (Table 2). Only the density surrounding Gly57 and Asp58 is displayed; Asp58 has been truncated beyond Cβ. Refinement of the occupancies is complicated by the overlap of many of the atoms in the three conformers. (b) Electron density corresponding to residues 56−58 in a $2|F_o| - |F_c|$ map of the reduced N137A mutant, computed after refinement using X-ray data measured at 140 K. $|F_o| - |F_c|$ difference maps of this region reveal no features larger than 3σ. The orientation, approximately perpendicular to the peptide Gly57-Asp58, was chosen to show the unique fit to a *trans* O-up conformation. Comparison of the shapes of the densities with those in panel b provides further evidence for the presence of a mixture of conformers in the oxidized mutant, N137A. The side chain of Met 56 is not shown.

in O-down conformations in the absence of intermolecular interactions, the *trans* O-up conformer becomes strongly favored when the flavin is reduced.

Oxidized and Reduced Forms of the Mutant D58P. Electron density corresponding to residues 56−59 in the oxidized form of the proline mutant is shown in Figure 8. The Gly57-Pro58 peptide is clearly *cis* and O-down in this structure, and the conformation resembles that in type VI turns in which the third position is occupied by *cis* Pro (Richardson, 1981; Lewis et al., 1973), except that Ψ58 is large (Table 4). Because of constraints on the Φ angle for proline, the Gly-Pro peptide must be *cis* if O57 points away from the flavin and *trans* if O57 is hydrogen-bonded to N5H. Otherwise, the backbone cannot form a chain reversal that follows the fold of the wild-type structure. The position of the Pro58 ring prevents formation of any hydrogen bonds between Asn137 and backbone atoms, and the neighboring Asn side chain turns away from the 57-58 peptide as shown in Figure 8b. The conformation of the Gly-Pro peptide appears to be unbiased by crystal contacts. Thus, the finding that the Gly57-Pro58 peptide rearranges to the *trans* O-up conformation when crystals are reduced (Figure 8c) provides unequivocal evidence that the conformation changes are driven by intramolecular interactions.

Mutants G57A, G57N, and G57D. For each of the mutants, G57A, G57N, and G57D, backbone orientations were assigned using the same criteria as in studies of wild type: the shapes of maps computed after refinements that omitted residues 57 and 58 and the features in difference maps after refinement of *cis* or *trans* conformations. Assignment of the *cis* or *trans* conformations is facilitated by the presence of a Cβ atom at 57, as the Cβ position is quite different in the two alternative orientations. In each oxidized flavodoxin, the 57 carbonyl is O-down, with the negative end of the C−O dipole directed away from the flavin ring. The peptides at 57 and 58 in the oxidized forms of the mutants G57A, G57N, and G57D are all *cis* and, like those of wild type, form two hydrogen bonds with the neighboring

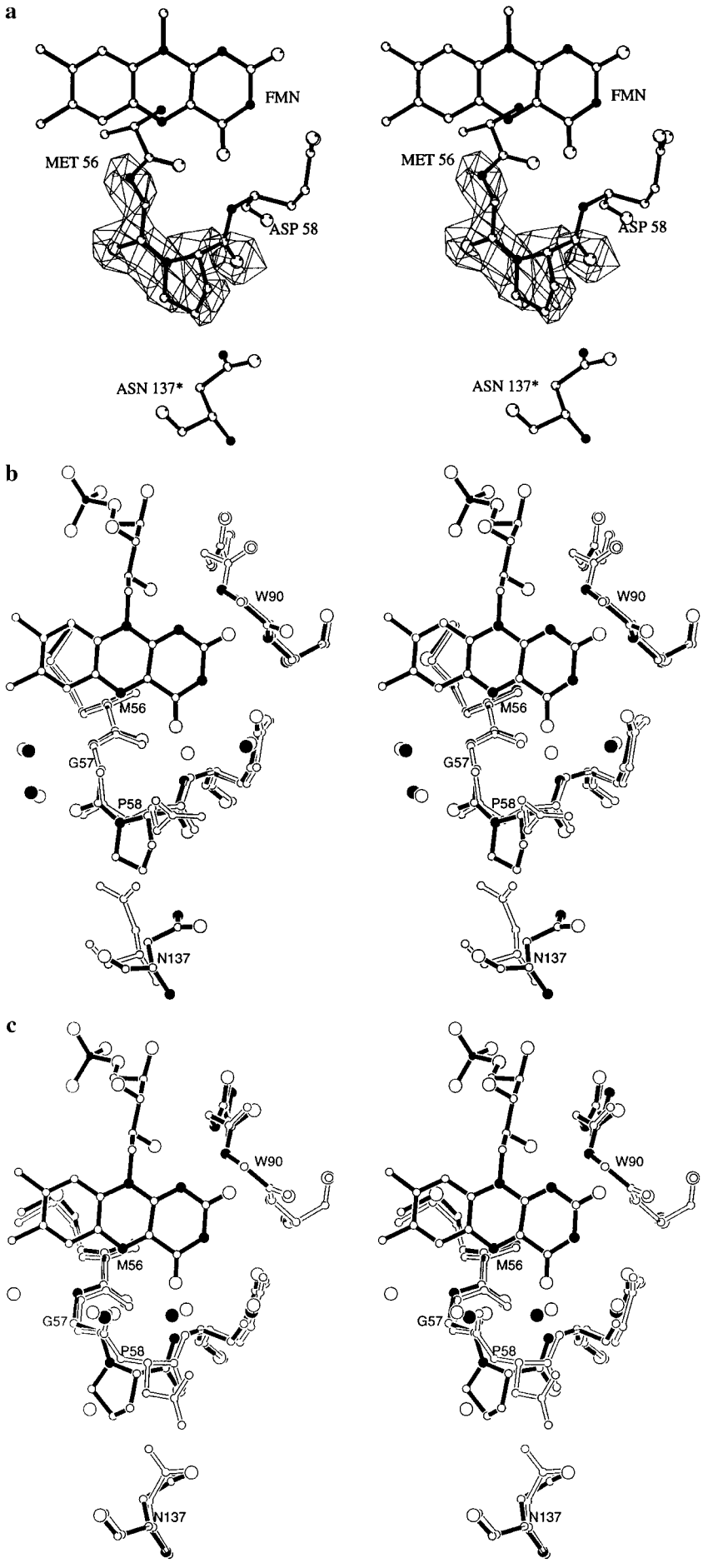
a
FMN
MET 56
ASP 58
ASN 137*
FMN
MET 56
ASP 58
ASN 137*
b
W90
M56
G57
P58
N137
W90
M56
G57
P58
N137
c
W90
M56
G57
P58
N137
W90
M56
G57
P58
N137

Table 4: Backbone Conformations at Residues 57 and 58

sequence and redox state	57-58 orientation	dihedral angles Φ, Ψ (deg)			
		Met56	residue 57	residue 58	Glu59
WT, ox[a]	*cis* O-down	−104, 172	−79, 128	−116, 110	60, 47
G57A, ox	*cis* O-down	−110, 173	−73, 126	−116, 109	58, 47
G57N, ox	*cis* O-down	−110, 175	−83, 131	−117, 107	64, 47
G57D, ox	*cis* O-down	−109, 176	−89, 136	−112, 111	62, 46
D58P, ox	*cis* O-down	−99, 180	−104, 142	−90, 103	51, 58
N137A, ox	*cis* O-down	−110, 166	−72, 122	−120, 116	58, 43
N137A, ox	*trans* O-down	−111, 178	−20, 105	57, 54	53, 55
N137A, ox	*trans* O-up	−122, 173	49, −127	−106,73	55, 54
G57T, ox	*trans* O-down	−108, 180	−34, 118	63, 40	58, 57
WT, sq	*trans* O-up	−125, 177	45, −131	−110, 84	59, 50
G57T, sq[b]	*trans* O-up	−121, 165	42, −114	−115, 85	56, 48
G57T, sq	*trans* O-down	−116, 178	−6, 99	55, 56	56, 55
WT, hq	*trans* O-up	−132, 174	51, −127	−117, 88	57, 56
N137A, hq[b]	*trans* O-up	−129, 175	48, −131	−108, 84	56, 50
G57D, hq	*trans* O-up	−126, 161	46, −114	−115, 88	50, 51
D58P, hq	*trans* O-up	−123, 177	47, −141	−77, 65	54, 58
G57T, hq	*trans* O-up	−128, 164	52, −99	−139, 87	57, 46
G57T, hq	*trans* O-down	−118, 174	1, 78	57, 80	50, 47
G57T, hq[b]	*trans* O-up	−123, 157	44, −98	−128, 84	56, 46
G57T, hq[b]	*trans* O-down	−130, 172	−10, 100	64, 47	55, 56

[a] Data collected at −10 °C. [b] Data collected at 140 K.

Asn137. Table 4 describes the conformations of the G57A, G57N, and G57D mutants. Like the wild-type protein, the G57D mutant rearranges to the *trans* O-up conformation when the flavin is reduced. The Φ, Ψ angles in reduced G57D are similar to those found in wild-type, but small differences in torsion angles at 56 and 57 appear to decrease overlap of Cβ with NH58. This contact is the dominant unfavorable feature of the type II′ turn (Venkatachalam, 1968; Richardson, 1981).

Mutant G57T. Of all the substitutions at position 57 that we have studied, threonine produces the most striking structural and functional changes from the wild-type protein. The threonine mutation alters the equilibria among oxidized conformers, strongly favoring the *trans* O-down form, which is the only conformation observed in the crystal structure. This conformer of Thr57-Asp58 resembles a classic type II β-turn. Significantly, the intermolecular packing in crystals of oxidized G57T is changed from that of wild type so that hydrogen bonding of O57 to the neighboring Asn137 is not possible (Figure 9a). We infer that the *trans* O-down conformation in oxidized G57T is dictated by intramolecular interactions and corresponds to the conformation adopted in solution. The observed preference for the *trans* O-down conformation deserves further study by computation; the relative energies of different threonine side chain orientations might be examined by computational methods such as those of Hagler et al. (1985). At first glance, it appears that the Oγ or methyl substituents in a *cis* O-down conformer of G57T would make close contacts with flavin or with other protein atoms over the entire range of the torsion about Cα−Cβ. In contrast, the threonine side chain is accommodated in the *trans* O-down conformation with no van der Waals contacts shorter than 3.4 Å between non-hydrogen atoms.

The dramatic shift of the ox/sq potential to −270 mV in the mutant G57T prompted us to undertake a structural analysis of the semiquinone form. Reduction at pH 6 at limiting concentrations of dithionite produced a crystal that by visual inspection was predominantly semiquinone (Materials and Methods), and data were collected at 140 K. Redox potentials predict that at pH 6 and 25 °C the fraction of semiquinone cannot exceed about 65%, and the electron densities were consistent with the presence of a mixture of O-up and O-down conformations. The fraction of the O-up conformer, estimated by refinement of occupancies, was approximately 60%. Our working assumption is that the observed structure corresponds to a mixture containing primarily semiquinone and oxidized states with the O-down conformer representing the oxidized form.

Two crystals of the G57T mutant, reduced in excess dithionite at pH 8−8.5, were analyzed; in one experiment, the data were measured at 4 °C, and in the other, the crystal was flash-frozen for measurements at 140 K. By visual inspection, both crystals contained residual semiquinone. The occupancy of the O-down conformer, estimated from final refinements including alternate *trans* O-up and *trans* O-down conformers, was 25−40%. Calculation of the expected mixtures of states at pH 8.5, extrapolating from the potentials of Table 3, shows that the fraction of the oxidized form should be about 15% when ∼1.5 electrons have been added and will decrease with further reduction. The large fraction of O-down species observed in the structure analyses raises the possibility that some of the reduced molecules adopt the

FIGURE 8: Structures of the oxidized and reduced forms of the mutant D58P. (a) Electron densities corresponding to residues 56−59 in an omit $|F_o| - |F_c|$ map of oxidized D58P flavodoxin establish the conformation of the *cis* Gly-Pro peptide and of the proline side chain. (b) Comparison of the structures of oxidized forms of wild-type flavodoxin and the D58P mutant. The molecular models were aligned by fitting the backbone atoms of residues 1−56 and 59−138. Intramolecular interactions of residues 56−59 are very similar in wild-type and D58P flavodoxins, but Asn137* is pushed away from the 57-58 peptide by the proline ring so that the intermolecular interaction with Asn137* is lost in the structure of the mutant. Side chains of Tyr88 and Trp90 and the FMN of the wild-type protein have been omitted in this and subsequent comparisons; the FMN groups coincide closely in the aligned structures. Solvents associated with the turn are shown; filled circles represent solvents in the structure of the mutant and open circles the solvents in the wild-type structure. (c) Comparison of the structures of the hydroquinone forms of wild-type flavodoxin and the D58P mutant. Conventions are the same as in panel b.

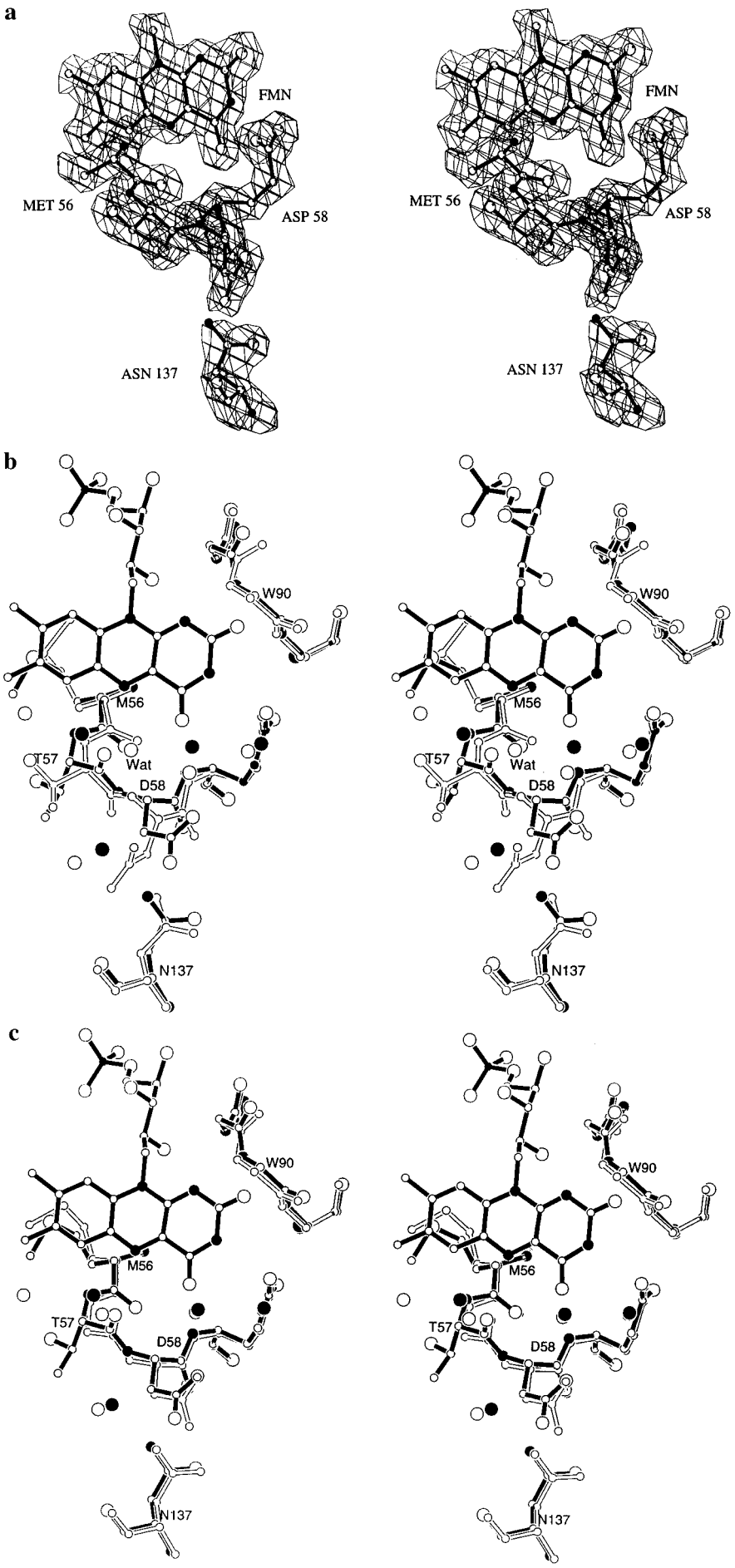
a
FMN
MET 56
ASP 58
ASN 137
FMN
MET 56
ASP 58
ASN 137
b
W90
M56
T57
Wat
D58
N137
W90
M56
T57
Wat
D58
N137
c
W90
M56
T57
D58
N137
W90
M56
T57
D58
N137

O-down conformation. Unfortunately, estimates of occupancies and estimates of the extent of reduction are not accurate enough to be certain of this conclusion. The O-down conformer, with the peptide flipped back, has been found in fully reduced *A. nidulans* flavodoxin (Luschinsky et al., 1991).

Models of the predominant O-up forms found in the reduced and in the semiquinone crystals of the G57T mutant reveal close contacts between the side chain and the backbone that increase the energy of this conformer, as expected for the second residue in a II′ turn (Figure 9c). Distances between the hydrogen of NH at position 58 and the Cβ of the threonine side chain are 2.37−2.42 Å. The distances between the threonine Oγ and Cγ and the hydrogens of NH57 and NH58 are also short. Significant changes in the Φ, Ψ angles at residue 57, relative to those of wild type (Table 4, Figures 9 and 10), move the Cβ atom of Thr57 out of the plane of the 57-58 peptide and appear to maximize the distances between backbone atoms and the Oγ and Cγ of Thr57. The mutant structure thus seems to compensate for the strain that is introduced by addition of a side chain; the Ψ angle in particular adopts less negative values in the reduced mutant G57T than in wild type (Table 4), relieving short contacts and moving the system downhill in energy (Anderson & Hermans, 1988). One consequence of the backbone torsion changes at residue 57 is a change in the orientation of the plane of the 57-58 peptide that can affect the geometry of hydrogen bonding between O57 and the flavin N5H (see Table 5). The branched side chain also restrains rotation about Cα−Cβ, since the alternate threonine rotamers would make close contacts with O56.

Turns at 56−59. Parameters for the three characteristic conformations that have been observed, *cis* O-down, *trans* O-down, and *trans* O-up, are listed in Tables 4 and 5. The Ramachandran plot of Figure 10 summarizes in a convenient way the differences between the three classes of conformers and also displays the effects of the mutations at positions 57 and 58. When the Gly57-Asp58 peptide is *cis* O-down, as found in oxidized wild-type flavodoxin, the O56−59N distance is short, suggesting strong 3_{10} O56−NH59 hydrogen bonding, whereas the 56O−N60 distance is significantly longer. The *trans* O-down conformation observed in the oxidized N137A and G57T mutants resembles a classic type II β-turn with 3_{10} hydrogen bonding. In contrast, in the *trans* O-up semiquinone and reduced forms, a backbone hydrogen bond between O56 and NH60 is preferred over that between O56 and NH59 (Table 5). The Φ, Ψ angles at Gly57 in the semiquinone and reduced forms are typical for type II′ turns, but the Ψ angle at Asp58 is near 90° rather than the 0° expected for such turns. The 56−60 region in reduced flavodoxins is best described as a three-residue turn (Milner-White & Poet, 1986; Sibanda & Thornton, 1985) with hairpin hydrogen bonding between residues 56 and 60 (Figure 4b). Distortions at residue 57 in reduced G57D and G57T and at residue 58 in D58P, implying differences in conformational energies as a result of mutation, are evident in the Ramachandran diagram.

Table 5: Hydrogen Bonding in the 56−60 Bend

		O56−NH59		O56−NH60	
structure	57−58 orientation	O···N distance (Å)	N−H···O deg angle[a]	O···N distance (Å)	N−H···O deg angle
WT, ox[b]	*cis* O-down	2.75	113.6	2.99	167.8
N137A, ox	*cis* O-down	2.66	107.1	2.91	170.5
N137A, ox	*trans* O-down	3.02	100.8	3.13	169.5
G57A, ox	*cis* O-down	2.67	111.5	2.92	167.4
G57N, ox	*cis* O-down	2.65	117.6	2.96	165.9
G57D, ox	*cis* O-down	2.71	115.0	2.96	166.9
D58P, ox	*cis* O-down	2.82	105.3	2.86	163.9
G57T, ox	*trans* O-down	2.87	112.6	3.06	163.2
WT, sq	*trans* O-up	3.16	104.1	2.93	169.1
G57T, sq[c]	*trans* O-up	3.10	99.0	2.96	163.8
WT, hq	*trans* O-up	3.18	99.7	2.82	162.7
N137A, hq[c]	*trans* O-up	3.11	100.3	2.80	168.8
D58P, hq	*trans* O-up	3.17	101.4	2.82	168.5
G57D, hq	*trans* O-up	3.24	91.4	2.95	164.5
G57T, hq	*trans* O-up	3.31	96.5	3.17	159.0
G57T, hq[c]	*trans* O-up	3.25	99.0	3.04	161.5

[a] The orientation of the 58−59 peptide, which appears to be influenced by the interaction between NH58 and the flavin O4, results in very nonlinear O56···HN59 angles. [b] Data collected at −10 °C. [c] Data collected at 140 K.

FMN−Protein Interactions and Solvent Contacts with the Flavin Binding Site

Protein−Flavin Contacts in Wild-Type and Mutant Flavodoxins. At the start of this study, it appeared that there would be a 1:1 correspondence between the bend conformation and the oxidation state of the flavin. We have instead found distributions of conformers in some oxidation states and, as expected, effects of mutations on the relative stabilities of these conformers. The observed sets of isoalloxazine−protein contacts are thus not uniquely determined by the oxidation state but depend on the conformation of the 56−59 bend, with interactions characteristic for the *cis* O-down, *trans* O-down, and *trans* O-up conformations. Distances between protein atoms and the flavin ring heteroatoms are compiled in Table 6, and information about the geometry of the CO57−N5H interaction is collected in Table 7.

The sets of protein−flavin interactions that are unique in structures with the O-up conformation involve O57. A

FIGURE 9: Structures of the mutant G57T. (a) Electron density corresponding to residues 56−59 in the crystal structure of the oxidized form of G57T. The methionine side chain has been truncated at Cβ; the drawing includes only the density contours that correspond to displayed atoms. The 57-58 peptide adopts a *trans* conformation resembling a type II turn. Refinement confirms that the Oγ atom, rather than the methyl group, is in contact with the flavin ring. The neighboring Asn137 side chain does not form hydrogen bonds to the 57-58 peptide. (b) Comparison of the structures of oxidized and reduced forms of the mutant G57T. The structure of the oxidized form is represented by open bonds and solvents; the reduced form is represented by filled bonds. In the structure of the oxidized mutant, the 57-58 peptide seems to shift laterally with respect to the flavin in wild-type flavodoxin. The interactions that drive this displacement are not obvious by inspection; packing of the threonine side chain and interactions of NH58 in the oxidized O-down structures are possible contributors. Rotation of the side chain of Met56 places the methyl group in the out position in the reduced form and appears to displace the solvent at N57. The solvent denoted Wat bridges NH58 and O4 in the oxidized *trans* O-down structure, and the solvent to its right moves toward O4 when the flavin is reduced. (c) Comparison of the structures of reduced wild-type and reduced G57T flavodoxins. Differences in torsion angles (Table 4) alter the position of Cα at position 57, relative to wild type, and the solvent near N57 is lost in the reduced form of the mutant protein. The methyl group of Met56 has swung away from the ribityl chain of FMN, as in the other structures of reduced flavodoxins.

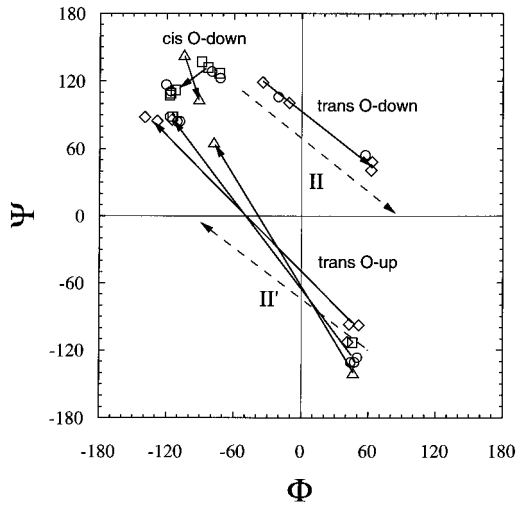

FIGURE 10: Ramachandran plot of the conformations of residues 57 and 58 in oxidized, semiquinone, and reduced flavodoxins from *C. beijerinckii.* Circles represent wild type and the N137A mutant, squares the G57A, G57N, and G57D mutants, diamonds the G57T mutant, and triangles the D58P mutant. Angles for the oxidized *cis* conformers (upper left) cannot be compared with any of the commonly observed β-turns; the *cis* Gly-Pro conformation, designated by triangles, differs somewhat from standard *cis* proline turns. The *trans* O-down conformers resemble the type II turn (shown as a dashed line). The cluster of *trans* O-up conformers shows the effects of the side chain at position 57 (lower right quadrant); the Φ angles are increased significantly in the Asp and Thr mutants. The conformation of the classic type II′ turn (dashed line) is displayed for comparison.

hydrogen bond between N5H and O57 forms in the semiquinone and reduced species where N5 is protonated. Special attention was paid to the N5−O57 interactions in each structure[2] (Table 7), because hydrogen bonding at N5H is expected to be critical in stabilization of the semiquinone state (Smith et al., 1977). Favorable electrostatic terms presumably make a major contribution to the N5H−O57 interaction. Geometric indices of strong hydrogen bonding include an N−H···O angle near 180° and good overlap of the hydrogen with the lone pair of the oxygen acceptor (Taylor & Kennard, 1984). In wild-type flavodoxins, the N−H···O angle is greater than 155°, consistent with strong hydrogen bonding, but the N5 hydrogen lies out of the plane of the 57-58 peptide by a rotation of ~70° around the C57−O57 bond (Table 7). This poor overlap is a consequence of the relative orientation of the peptide and flavin planes and the large angle between them. In the mutant flavodoxins, particularly G57T, the N−H···O angles and other features of the N5H−O57 geometry are altered slightly in directions consistent with weakened N5H···O57 interactions (Kabsch & Sander, 1983). Formation of the N5H···O57 bond in the O-up conformers also comes with a built-in penalty; O57 and O4, with partial negative charges, are in van der Waals contact in the O-up semiquinone and hydroquinone structures. The C4−O4 and C57−O57 dipoles are arranged in an offset head-to-head manner as can be seen in Figure 4b and other figures displaying structures of reduced flavodoxin mutants. In the structures analyzed in Table 6, the longer O4−O57 distances are associated with longer N5−O57 distances. Variations in this pair of interactions result from combinations of rotation and tilt of the 57-58 peptide plane with respect to the flavin plane, which depend in turn on (and are very sensitive to) the Φ, Ψ angles at residues 56 and 57. In this way, distortions in the conformation of the backbone, discussed in the preceding section, may be linked to changes in protein−flavin interactions.

Comparisons among structures of the same conformers (*trans* O-up, *cis* O-down, or *trans* O-down) reveal only small changes in protein−heteroatom distances as a result of sq → hq reduction or as a consequence of the mutations that we have studied. Significant effects of flavin reduction on hydrogen bonding energies are expected from the redistributions of charge in the isoalloxazine ring (Hall *et al*., 1987a,b) that accompany reduction, but these changes are not apparent in the distances separating N1, O2, or O4 from protein donors. Variations in flavin−protein interactions involving O57, observed after refinement of the two structures of reduced G57T flavodoxin, one based on data collected at 4 °C and the other at 140 K, are puzzling. Different temperatures and different solvent interactions might contribute to these variations, but reduced wild-type and reduced N137A structures, also based on data collected at different temperatures, show very similar isoalloxazine−protein interaction geometries.

To study the N5H−protein interactions in a different way, we measured the p*K* of N5H in the semiquinone form of the mutant G57T.[3] The p*K* of N5H in flavodoxin semiquinone, relative to that of free FMN semiquinone in water, is related to the strength of the N5H−O57 interaction (Smith et al., 1977). In wild-type *C. beijerinckii* flavodoxin semiquinone, the N5H p*K* is increased to >13 from the value of 8.5 for free FMN (Ludwig et al., 1990; this work). Spectral changes of the G57T mutant measured after mixing of concentrated high-pH "buffers" with the neutral blue semiquinone showed rapid formation of anionic red semiquinone with a p*K* near pH 11.3. This p*K* decrease of at least 2 pH units (>2.6 kcal/mol) seems larger than might be expected from the comparatively subtle differences in the geometry of interactions in the vicinity of the N5H group, discussed above, and suggests that titration of N5H may be associated with other changes in addition to removal of the proton. If the 57-58 peptide reorients upon deprotonation, then the p*K* shift would also be correlated with the stability of the O-up conformation.

Solvation of the Isoalloxazine Ring and Rearrangement of the Met56 Side Chain. Compared with other flavodoxins, the isoalloxazine in clostridial flavodoxin is remarkably accessible to solvent (Ludwig & Luschinsky, 1992). The principal interactions of solvent with the flavin ring and residues 56−59 are shown in Figure 4b and compiled in Table 8. Solvents are associated with the backbone atoms of Gly57 and Asp58 at sites that vary depending on the conformation of the 57-58 peptide (see Figures 8 and 9), and a channel filled with solvents penetrates to O2. A firmly bound buried solvent is associated with O2 in every structure, and two other solvents are bound near OE1 of Glu59 in the

[2] In refinement of the models used for comparisons of mutants with wild-type protein, the polar N5 hydrogen was added to the semiquinone and reduced flavins, but explicit H bond potentials were not employed.

[3] Because the charge at the N5H atoms is decreased by addition of the second electron (Hall, 1987), the N5H···O57 hydrogen bond is expected to be weaker in the reduced than in the semiquinone state. Measurements of the effects of the protein on the deprotonation of N5H in fully reduced isoalloxazines are not possible since the p*K*s are too high to determine.

Table 6: Interactions of the Isoalloxazine Oxygen and Nitrogen Atoms[a]

structure	orientation	N1−N89	O2−N89	O2−N91	N3−OE159	O4−N59	N5−O57	O4−O57
WT, ox[b]	*cis* O-down	3.05	3.10	2.71	2.79	2.90		
N137A, ox[c]	*cis* O-down	3.11	3.02	2.83	2.84	2.88		
N137A, ox[c]	*trans* O-down	3.11	3.04	2.85	2.92	3.14		
G57D, ox	*cis* O-down	3.11	3.04	2.76	2.91	2.97		
D58P, ox	*cis* O-down	3.13	3.09	2.82	2.86	2.93		
G57T, ox	*trans* O-down	3.03	3.00	2.76	2.85	3.08[e]		
WT, sq	*trans* O-up	3.00	2.95	2.78	2.84	2.84	2.82	3.25
G57T, sq[c,d]	*trans* O-up	3.03	3.02	2.76	2.89	2.73	2.76	3.31
WT, hq	*trans* O-up	2.96	3.05	2.71	2.96	2.76	2.99	3.51
N137A, hq[d]	*trans* O-up	3.00	3.06	2.72	2.92	2.68	2.99	3.50
G57D, hq	*trans* O-up	2.96	2.98	2.79	3.00	2.79	2.94	3.31
D58P, hq	*trans* O-up	3.06	2.98	2.76	2.83	2.84	2.95	3.10
G57T, hq[c]	*trans* O-up	2.91	2.95	2.76	2.88	2.84	3.10	3.71
G57T, hq[c,d]	*trans* O-up	2.99	3.06	2.72	2.95	2.66	2.77	3.20

[a] Distances in angstroms. [b] Data collected at −10 °C. [c] Structure model includes more than one conformation of residues 57 and 58. [d] Data collected at 140 K. [e] A relatively long O4−N59 distance is found in oxidized G57T, where O4 also interacts through a water bridge with NH58.

Table 7: N5H−CO57 Interaction in O-Up Semiquinone and Reduced Structures

sequence	N···O−C angle	N−H···O angle	angle H out-of-plane (deg)	peptide−FMN angle (deg)
wild type, sq	139.5	165.6	−60	43.2
wild type, hq	132.7	156.4	−74	46.5
N137A, hq	133.9	155.6	−71	43.8
D58P, hq	141.6	172.4	−24	36.8
G57D, hq	125.4	161.3	−61	47.3
G57T, sq	131.3	157.4	−68	42.3
G57T, hq (1)	111.0	153.3	−83	60.2
G57T, hq (2)	115.0	144.6	−69	49.0

outer part of the channel. Another water is associated with Trp90NE1 (see below). In the oxidized G57T mutant (Figure 9), a solvent bridges NH58 and the flavin O4 at a site that appears to be a marker for the *trans* O-down conformer. Mutation of Gly57 perturbs the distribution of solvents in the vicinity of the mutation site. For example, the positions of the Asp and Thr side chains in the reduced forms of the G57T and G57D mutants obstruct or alter the binding of solvent near N57 (Figures 8 and 9).

Solvents bound to reduced wild-type and mutant flavodoxins may be especially important for solvation of the anionic reduced flavin (Figure 4b) and may help to account for the high sq/hq and ox/hq (two-electron) potentials of *C. beijerinckii* flavodoxins, relative to those of other flavodoxins (Ludwig & Luschinsky, 1992; Swenson & Krey, 1994; Stockman et al., 1994). One solvent site near O4 is strongly dependent on the oxidation state of the flavin. A water associated with NE1 of Trp90 in the oxidized structures moves closer to O4 when the flavin is reduced. In the reduced flavodoxins, this water appears less mobile and is coordinated by O4, by the ring NE1 of Trp90, and by the carboxyl of Asp58 (Figure 4b). This site is occupied in all of the reduced mutant flavodoxins but has two rather than three ligands in the reduced mutant D58P. In all structures except the D58P mutant, a solvent is bound at NH58 in the O-up conformers of reduced or semiquinone flavodoxins, and in most of the reduced flavodoxins listed in Table 8, a solvent is also weakly associated with O57 in the O-up conformation.

Reduction of the flavin is accompanied by changes at Met56 in wild-type and mutant flavodoxins. The backbone Φ angle at Met56 decreases by 15−25° when the flavin is reduced, and 57-58 adopts the O-up conformation (Table 4). These torsion changes at the Met56 backbone move O56 away from C57, avoiding eclipse of the C56−O and the Cα57−C bonds. In the semiquinone and reduced structures, rotation about the Cγ−S bond swings the methyl group of Met56 from a position near the ribityl side chain and the flavin C9 to a more solvent-exposed location where it adjoins the 7-CH_3 substituent of isoalloxazine. This reorientation of the methyl group alters the overlap of the sulfur orbitals with the flavin ring. Rotation of the methyl group seems to be complete in the wild-type semiquinone structure, which is based on data from crystals grown from solutions of the semiquinone form; there is no difference density adjoining O55. However, difference densities are observed near O55 in several structures, at positions corresponding approximately to the location of the Met56 CH_3 group in oxidized flavodoxin. These may represent water or the alternate position of the 56 methyl group but are too far from the sulfur to be sulfoxide oxygens. In the semiquinone form of G57T, this difference peak is likely to correspond to the methyl group in molecules which remain oxidized. Water placed in the difference density near O55 in wild-type fully reduced flavodoxin refines to reasonable occupancies, but the methionine sulfur remains at a position about 2.5 Å from the putative water oxygen, too close for OH···S hydrogen bonding. Thus, the evidence that solvent occupies this site in the structure of wild-type flavodoxin is not convincing. In contrast, solvent may enter this site in fully reduced G57T mutants, forming hydrogen bonds to O55 and to the methionine sulfur atom.

DISCUSSION

Protein−cofactor interactions modulate the oxidation−reduction potentials of bound prosthetic groups such as FMN. The connection between potentials of flavodoxins and free energies of FMN−protein interactions can be cast in the formalism of thermodynamic cycles that relate shifts in potential, relative to free FMN, to oxidation-state-dependent differences in the free energies of FMN−apoprotein association (Dutton & Wilson, 1974; Mayhew & Ludwig, 1975) (see Figure 11). The peptide rearrangement that accompanies reduction to the semiquinone form in *C. beijerinckii* flavodoxin provides a versatile device for manipulation of the ox/sq potential. The conformation change can act in two ways, first by altering flavin−protein contacts and second

Table 8: Solvent Interactions with Isoalloxazine and Adjoining Residues[a]

crystal	57−58 orientation	N57	O57 (up)	O57 (down)	N58	OE159	NE1-90	O4	O2
WT, ox[b]	*cis* O-down	3.10		2.83		2.83	2.81	3.4	3.31
		0.7/15.4		0.6/13.4		1.0/28.3	0.9/29.5	0.9/29.5	1.0/6.5
G57A, ox	*cis* O-down	3.31		2.80		2.77	2.84	3.77	3.32
		1.0/40.8		0.4/2.0		1.0/33.5	0.8/17.6	0.8/17.6	1.0/2.0
G57N, ox	*cis* O-down	*d*		2.74		2.72	2.73	3.20	3.15
				0.7/31.0		0.9/42.7	0.8/38.3	0.8/38.3	1.0/8.9
G57D, ox	*cis* O-down	3.28[e]		2.81		2.85	2.72	3.82	3.29
		0.7/19.9		0.6/20.7		1.0/35.6	0.8/26.8	0.8/26.8	1.0/5.6
G57T, ox	*trans* O-down	2.92		2.83[g]	2.79[g]	2.87	3.53	2.85[g]	3.26
		0.6/52.0		0.9/35.6	1.0/29.0	0.9/27.8	0.8/49.6	1.0/29.0	1.0/7.8
D58P, ox	*cis* O-down	2.84		2.93		2.88			3.30
		0.7/16.1		0.7/16.8		0.8/21.0			1.0/5.8
WT, sq	*trans* O-up	3.07	2.90		2.80	2.92	2.84	2.79	3.21
		0.7/14.2	1.0/42.1		1.0/28.9	1.0/29.1	0.6/21.4	0.6/21.4	1.0/9.7
G57T, sq[c]	*trans* O-up		2.72		3.14	2.81	2.88	2.81	3.19
			0.6/30.6		1.0/21.0	1.0/15.4	0.6/6.5	0.6/6.5	1.0/5.9
WT, hq	*trans* O-up	3.06	2.89[f]		3.07	2.81	2.92	2.71	3.23
		0.5/8.0	1.0/52.8		1.0/33.5	0.8/16.4	0.8/17.6	0.8/17.6	1.0/7.2
N137A, hq[c]	*trans* O-up	3.04	2.88		2.88	2.82	3.01	2.68	3.06
		1.0/17.1	1.0/37.8		1.0/11.2	0.9/10.1	0.8/2.2	0.8/2.2	1.0/2.0
G57D, hq	*trans* O-up		2.84		3.03	2.87	3.05	2.58	3.26
			1.0/44.0		1.0/42.9	0.8/23.3	0.6/10.2	0.6/10.2	1.0/9.4
D58P, hq	*trans* O-up	3.13	2.90			2.89	3.11	2.61	3.27
		0.8/17.6	1.0/39.0			1.0/22.4	0.6/15.4	0.6/15.4	1.0/5.1
G57T, hq	*trans* O-up		2.70		*d*	2.75	2.88	2.67	3.32
			1.0/45.5			1.0/31.0	0.4/4.7	0.4/4.7	1.0/7.7
G57T, hq[c]	*trans* O-up		2.56		2.63	2.75	2.93	2.69	3.23
			1.0/34.5		0.7/32.2	0.8/11.2	0.6/4.5	0.6/4.5	1.0/4.2

[a] Waters are identified by their nearest protein neighbors, except for the water that bridges O4 to NH58 in G57T and the single water associated with both O4 and NE1-90. Distance in angstroms; occupancy/temperature factor in second line. [b] Data collected at −10 °C. [c] Crystal frozen at 140 K. [d] Not detectable in the structure based on data collected at 4 °C. [e] Also associated with the side chain of Asp57. [f] Less scattering than required for assigning a solvent position; listed for comparison with the other structures. [g] A site that is unique to the *trans* O-down conformation in G57T.

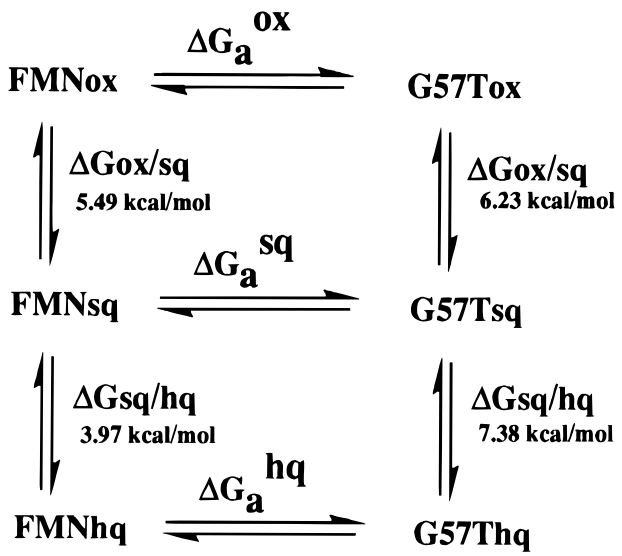

FIGURE 11: Thermodynamic cycles describing the potential shifts resulting from binding of FMN to the G57T mutant protein. The additional free energy for full reduction of G57T, 2.3 kcal/mol relative to that of wild type, is equivalent to a decrease of a factor of ~60 in the ratio of association constants, K_a (hq)/K_a (ox).

by changing the conformational energy of the protein itself. The present study has examined the conformations and flavin interactions of residues 56−59 in oxidized, semiquinone, and reduced clostridial flavodoxins, in order to understand how conformation changes in this region of the protein may affect the redox potentials.

To interpret the results, it is convenient to define two kinds of free energies that contribute to control of potentials. The first energy term, ΔG_c, refers to the energy difference between conformers of the apoprotein, e.g. the difference between the *trans* O-up and *trans* O-down conformers. The second energy term, ΔG_i, refers to the energy of interaction of FMN (ox, sq, or hq) with the appropriate conformer(s) of the apoprotein. [see the scheme in the Appendix (Figure 13)]. In this partition of the energies, the apoprotein is a virtual structure with the atomic coordinates found in the crystal structures of the holoproteins, but with FMN not bound. Thus, the semiquinone apoprotein has the atoms of residues 57 and 58 in the O-up conformation. ΔG_c and ΔG_i are not readily separable in experiments, but division into two virtual steps in this fashion allows correlations of ΔG_c with model and computational studies of protein conformations.

The conformational and interaction energies have been manipulated by mutation of residues Gly57 and Asp58 that are involved in redox-linked rearrangements. Gly57 was chosen as a site for mutation because structures for the wild-type semiquinone had shown that it adopts a conformation that is fully allowed only for glycine. From computational (Venkatachalam, 1968) and empirical (Smith & Pease, 1980) studies of peptide conformation, substitutions for this Gly were predicted to produce substantial changes in ΔG_c, increasing the energies for the rearrangement of the 57-58 peptide to the O-up conformation. Mutation of Asp58 to proline was partly prompted by the finding that the wild-type Gly57-Asp58 peptide could adopt the *cis* conformation, suggesting that it might be possible to exploit known differences in the relative stability of *cis* and *trans* forms of proline and non-proline peptides to study the control of redox potentials. Although isoalloxazine−protein contacts are made by backbone rather than by side chain atoms of residues

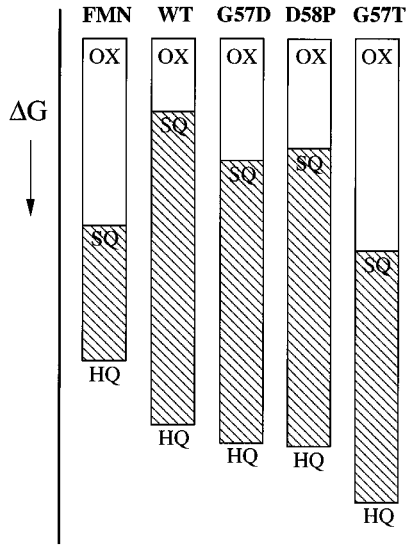

FIGURE 12: Free energy ladders that show the relative costs of adding each electron for FMN, WT, G57D, and G57T (left to right). Free energy increases in the downward direction along the ordinate. The total length of the ladders is proportional to the overall free energy for two-electron reduction, which is split into contributions for each step. In FMN, ΔG for addition of the first electron is larger than that for addition of the second electron; however, in wild-type *C. beijerinckii* flavodoxin, the first reduction has a small free energy, and the two one-electron potentials are well-separated. Energies of the oxidized forms have arbitrarily been made equal. The energy ladder for G57T is significantly longer than that for wild type, but it is not clear whether this implies that the oxidized form of the mutant is more stable than wild type. Measurements of association constants for oxidized FMN would be helpful in aligning the energy ladders with one another but cannot establish the relative energies of oxidized forms unambiguously because mutation may affect the energies and conformations of the apoprotein.

57 and 58, substitutions at these sites nevertheless do modulate potentials, as we had anticipated.

Table 3, which lists the potentials and free energies for reduction of FMN in wild-type and mutant flavodoxins, shows that the mutations we have studied have large effects on the ox/sq potential, as might be expected since the conformation change occurs at this step. Energy ladders (Figure 12) display the relative energies associated with reduction of wild-type and mutant proteins and demonstrate graphically the decreased propensity of mutants to form the semiquinone. In the mutants D58P, G57A, G57D, and G57N, the free energies for reduction to semiquinone increase by about 1.3 kcal/mol. The G57T mutant shows a similar pattern, but with a much larger energy increase of 4.1 kcal/mol. Although the effects on the sq/hq equilibria are smaller in magnitude, the mutations that were studied all make addition of the second electron easier than in the wild-type protein. The free energy for the reduction of sq $\rightarrow$ hq decreases by 0.7 kcal/mol for the mutants G57A/D/N and D58P and by 1.8 kcal/mol for G57T. These increases in the sq/hq potentials are not fully understood. They appear to come from effects of mutation on ΔG_i terms since, with the possible exception of the mutant G57T, residues 57 and 58 do not change conformation when the second electron is added to the flavin (see below).

Structure analyses reveal three patterns for conformations of the 57-58 peptide in the mutants. G57D is most like wild type. In the oxidized state, the Asp57-Asp58 peptide is *cis* O-down in crystals, where Asn137 of a neighboring molecule helps to stabilize this conformation. We assume that, in the absence of interactions with Asn137*, the oxidized form of this mutant, like wild-type flavodoxin, is a mixture of conformers. The Asp57-Asp58 peptide rearranges to the *trans* O-up conformation on reduction. In contrast, the D58P mutant is all *cis* O-down when bound FMN is oxidized and rearranges to *trans* O-up on reduction. Finally, the oxidized G57T mutant is *trans* O-down and rearranges to *trans* O-up when converted to the semiquinone form. Crystal structures have not been determined for the semiquinone forms of the D58P and G57D mutants, but all our studies of flavodoxins have found that, if the fully reduced (hydroquinone) structures adopt the O-up conformation, then so do the semiquinone forms. Because they exhibit qualitative and quantitative differences in structure and redox properties, each of the mutants, D58P, G57D, and G57T, will be considered in turn.

D58P Mutant. In the D58P mutant, the free energy change for the *cis*−*trans* isomerization of the Gly-Pro peptide that accompanies reduction to the semiquinone should differ from the free energy change for the rearrangement of the wild-type Gly-Asp peptide. A shift in potential is thus expected from this difference in ΔG_c. The energy for *cis*−*trans* isomerization in isolated X-Pro peptides has been computed to be −0.5 kcal/mol (Maigret et al., 1970; Eberhardt et al., 1992). In comparison, values of −2.0 to −2.5 kcal/mol have been calculated for peptides not containing proline (Jorgensen & Gao, 1988; Herzberg & Moult, 1991). Although the energy change associated with *cis*−*trans* isomerization may depend on the context of a particular protein (Hodel et al., 1995; Mayr et al., 1994), the computed values of −0.5 and −2.25 kcal/mol predict a change in the conformational energy for the oxidized to semiquinone rearrangement ($\delta\Delta G_c^{ox/sq}$) of approximately 1.8 kcal/mol when *cis* Gly-Pro is substituted for *cis* Gly-Asp. The observed difference of 1.4 kcal/mol in the ox/sq potential suggests that $\delta\Delta G_c$ makes important contributions to the decrease in the ox/sq potential observed in the D58P mutant. The observed potential changes will also include the effects on ΔG_c of the mixture of conformers in wild type, along with perturbations to ΔG_i from altered FMN−protein interactions. In the oxidized state, differences in ΔG_i can arise because the 57-58 peptide in the oxidized mutant D58P is all *cis* while wild type, modeled by the mutant N137A, is a mixture of three conformers.

Peptide isomerization in the D58P mutant is of interest for additional reasons. The *cis*−*trans* conversion that occurs in the crystal is significant for the present study because it takes place in the absence of interactions with neighboring molecules. Studies of the D58P mutant thus confirm that intramolecular effects of reduction (addition of $H^+ + e^-$) drive the peptide from O-down to O-up. It is intriguing that introduction of proline does not lock the Gly-Pro peptide into a single conformation. The D58P mutant is one of a few examples of *in situ cis*−*trans* isomerization at proline; probably the best-studied case is staphylococcal nuclease (Hinck et al., 1993; Alexandrescu et al., 1989; Fox et al., 1986). Preliminary data indicate that one-electron oxidation of semiquinone D58P flavodoxin in solution, which is presumably accompanied by *trans*−*cis* isomerization, is rapid on the stopped-flow time scale. Further studies of the rates and energetics of rearrangement in the D58P mutant would be valuable for comparison with the X-ray results and for

comparison with other investigations of X-Pro peptide stability (Mayr et al., 1994) and rates of isomerization. Recent estimates of activation energy barriers have varied from 13 kcal/mol [cited in Schulz and Schirmer (1979)] to about 20 kcal/mol (Cheng & Bovey, 1977; Eberhardt et al., 1992).

G57D Mutant. We determined the structure of the fully reduced mutant G57D as the prototype for the series of mutants, G57A/N/D. These mutations at Gly57 were all expected to make addition of the first electron more difficult by increasing the nonbonded interaction energy in the O-up conformer, thereby disfavoring the transition to O-up (increasing $\Delta G_c^{ox/sq}$). Computations on dipeptide models have led to a range of values for the magnitude of the increase in energy incurred by substitution of "simple" side chains such as Ala in the O-up conformation observed at Gly57 in wild-type semiquinone. Early estimates of the energy difference between Ala and Gly residues in the region corresponding to the O-up (or II′ turn) conformation (Peters & Peters, 1981) were as large as 8 kcal/mol, but these were computed for peptides *in vacuo*. From more recent Ramachandran maps for the alanine dipeptide (Anderson & Hermans, 1988) and other calculations (Yang et al., 1996; Pettitt & Karplus, 1985; Weiner et al., 1984), one estimates a smaller effect of glycine replacement by alanine, 2.5 kcal/mol or less. In our studies of the mutants G57A, G57N, and G57D, the introduction of a side chain shifts the ox/sq potential in the expected direction but by less than the magnitudes cited for Ala substitution in simple models. Reduction is disfavored by an average of about 60 mV (1.4 kcal/mol). As in the D58P mutant, the potential shifts induced by the change in sequence also include contributions from altered flavin−protein interactions. For the G57D mutant, the mixture of conformations in the oxidized state will differ from that in oxidized wild-type flavodoxin, since the side chain destabilizes the O-up conformer. Thus, interactions with FMN will not be the same as in wild type ($\delta\Delta G_i^{ox}$ terms may contribute to the potential shifts). In summary, the impression from analyses of the D58P and G57D mutants is that the dominant effects of these mutations are on ΔG_c and that changes in ΔG_i are secondary contributors to the potential shifts.

G57T Mutant. Introduction of the branched side chain of threonine at position 57 has a much larger effect on the potentials and structures than does the aspartate substitution. The more dramatic changes resulting from the threonine substitution are visualized in the energy ladder of Figure 12. In contrast to wild type, the first and second electrons are added to the G57T mutant at potentials that differ by only 50 mV at pH 7 (see Figure 3), and the mutant is more difficult to reduce to semiquinone than is wild type. The two-electron midpoint potential of the G57T mutant is significantly decreased compared to that of wild-type flavodoxin so that the free energy of the overall two-electron reduction increases by 2.3 kcal/mol.

Substitution of the threonine side chain has major effects on the relative energies of the *cis* O-down, *trans* O-down, and *trans* O-up conformations of the 57-58 peptide. In contrast to wild type, the *trans* O-down form is the only conformation found in the oxidized state. The O-up conformer still dominates in the presence of the FMN semiquinone, but we suspect that the free energy increment for substitution of the threonine side chain in the O-up conformer is larger than for substitution of alanine or aspartate (Janin et al., 1978). All the evidence indicates that the ΔG_c associated with the conversion between the oxidized and semiquinone conformers is significantly more positive than in wild-type flavodoxin. The threonine mutation may in fact have introduced an energy gap between oxidized (*trans* O-down) and semiquinone (*trans* O-up) conformers close to that required to "lock"' the molecule in the O-down conformation.

The flavin−protein interaction terms are also more affected by the Gly57Thr substitution than by the other mutations. In the oxidized state, the *trans* O-down conformer of G57T makes FMN contacts that differ from those of the *cis* O-down and *trans* O-up conformers that constitute most of the species in the oxidized wild-type structure. The semiquinone and reduced (hydroquinone) O-up structures are not so obviously different from wild type, and the changes in geometry that can be detected are relatively subtle (Tables 6 and 7). In this case, the N5H p*K* provides an independent measure of the effects of mutation on the semiquinone state. The proton at N5 is more weakly bound in the mutant than in wild type, with a p*K* difference corresponding to at least 2.6 kcal/mol. The lower p*K* is consistent with the poorer geometry for hydrogen bonding between N5H and O57 in the semiquinone form of G57T, relative to wild type, and may also be correlated with decreased stability of the O-up conformation. In summary, the structures, together with the potentials and measurements of the N5H p*K* in the semiquinones, suggest that replacement of Gly57 by threonine has significantly altered the energies of protein−FMN interactions in both the oxidized and semiquinone states, as well as the energies associated with the conformation of the 56−59 bend. However, it is difficult to separate the overall effects of the threonine substitution into contributions to ΔG_c and ΔG_i terms.

Effects of Mutation on the sq/hq Potentials. The increases in sq/hq potential that result from all the mutations reported here are not easy to rationalize. Changes in the sq/hq potential are smaller than those in the ox/sq potential but are clearly significant. As shown in the Appendix, these increases in sq/hq potential cannot be explained by effects of mutation on ΔG_c for the ox/sq conversion, but require changes in at least one of the energies, $\Delta G_c^{sq/hq}$, ΔG_i^{sq}, or ΔG_i^{hq}. There is no compelling evidence from the X-ray data (Tables 6 and 7) for differential effects of mutation on the flavin−protein interactions in semiquinone and hydroquinone structures that might explain why the semiquinone to hydroquinone conversion is easier than in wild type. We tentatively conclude that the energies associated with protein−flavin interactions in the semiquinone state are somehow more affected by the small structural distortions accompanying mutation than are interactions in the fully reduced state (in the notation of Figure 13, $\delta\Delta G_i^{sq}$ is more positive than $\delta\Delta G_i^{hq}$). Weaker flavin−protein interactions in the hydroquinone state or enhanced mobility of the fully reduced protein (Leenders et al., 1993, 1994) might account for a smaller sensitivity of the hydroquinone forms to mutation. A further implication is that interaction energies in the semiquinone may be exquisitely sensitive to rather small changes introduced by conservative substitutions in the FMN binding site [e.g. Zhou and Swenson (1995)]. Finally, in the case of G57T, the X-ray data hint that partial reversion (flip-out) of the Thr57-Asp58 peptide occurs in the fully reduced form. A reversion to O-down has been observed

in the reduced flavodoxin from *A. nidulans* (Luschinsky et al., 1992). A significant energy associated with backbone rearrangement might then contribute to the sq/hq potential. It would be helpful to determine a structure for a G57T crystal in which FMN is fully converted to the hydroquinone state.

Control of the ox/sq Potential in Wild-Type C. beijerinckii Flavodoxin. An important result of this work is the recognition that oxidized *C. beijerinckii* flavodoxin exists as a mixture of conformers of the Gly57-Asp58 peptide: *cis* O-down, *trans* O-down, and *trans* O-up. This finding implies that the conformational energies of these species, in the context of the oxidized holoprotein, are not very different; that is, $\Delta G_c^{ox/sq}$ is small in the wild-type protein. Molecular dynamics and free energy perturbation calculations (Scully & Hermans, 1994) are attractive approaches for further examination of the energies of these conformers. From the structures and properties of the mutants, one can conclude that the conformation change has its principal impact on the energy of semiquinone formation and is required to form strong interactions in the semiquinone state. The ox/sq potential will be high if the energy of the semiquinone conformation is minimized and protein−flavin interactions in the semiquinone state are optimized. This optimal situation may prevail in *C. beijerinckii* flavodoxin; no penalty is paid for conversion to the "desirable" O-up type II′ semiquinone conformation when glycine is the residue at position 57. In several flavodoxins, including the proteins from *M. elsdenii* and *D. vulgaris*, and perhaps others among the sequences that have been determined (Ludwig & Luschinsky, 1992), a conserved glycine residue in the loop adjoining the N5 edge of the flavin ring may also play a critical role in regulating the ox/sq potentials.

ACKNOWLEDGMENT

We thank Dr. D. P. Ballou for carrying out and analyzing the pH jump experiments, which were performed in his laboratory, and we are grateful to David M. Hoover for his assistance in freezing the crystals for low-temperature X-ray measurements. Many of the drawings were prepared with the program MAXIM, written by Mark Rould.

APPENDIX

The effects of mutation on energies can be analyzed using the cycles shown in Figure 13. This scheme divides the effects of the protein into two virtual processes, one involving energy changes in the protein itself and the other involving FMN−protein interactions. The vertical steps on the left define energies associated with conformation changes in the protein (ΔG_c). Each PROTEIN$^{(i)}$ is an apoprotein whose structure is defined by the atomic positions observed in the crystal structure of the holoprotein. The horizontal steps on the right define energies for interaction, ΔG_i, between the given oxidation state of free FMN and the corresponding apoprotein conformer, PROTEIN$^{(i)}$. The measured *shifts* in potential, ΔE, relative to free FMN, appear in the right-hand vertical limbs and equal the sum of the steps in each box; e.g. $\Delta E(ox/sq) = \Delta G_c^{ox/sq} + \Delta G_i^{sq} - \Delta G_i^{ox}$.

The simplest consequence of the D58P, G57A, G57N, and G57D mutations would be an effect restricted to $\delta\Delta G_c^{ox/sq}$, a perturbation of the energy associated with rearrangement of the 57-58 peptide. In this case, the only impact of the mutations would be on the protein−protein interactions that are altered when the conformation changes; energies associated with flavin−protein interactions, ΔG_i, would be unperturbed by the mutations. Adding contributions around the upper and lower thermodynamic boxes for the one-electron reductions shows that the change in $\Delta G_c^{ox/sq}$ resulting from mutation, $\delta\Delta G_c^{ox/sq}$, will shift the ox/sq potential by an amount corresponding to the increase in the energy associated with the conformation change but will not alter the sq/hq potential. Changing the sq/hq potential requires an effect of mutation on at least one of the energies in the lower cycle, $\Delta G_c^{sq/hq}$, ΔG_i^{sq}, or ΔG_i^{hq}.

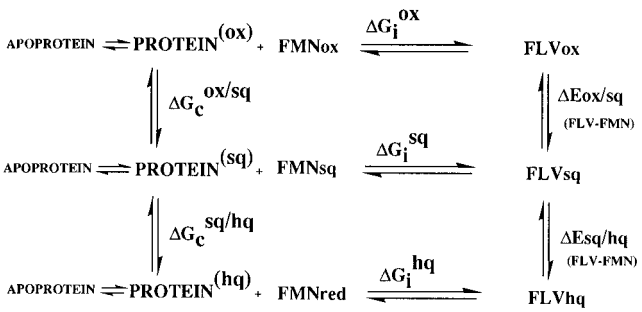

FIGURE 13: Thermodynamic scheme that describes how free energies of FMN reduction are perturbed when FMN is bound to flavodoxin. Apoprotein (far left) is in equilibrium with a hypothetical species, PROTEIN$^{(i)}$, which has the conformation characteristic for the ox, sq, or reduced state of the holoprotein but is not bound to FMN. ΔG_c is the energy difference between the PROTEIN$^{(i)}$ structures. Free energy changes associated with the interaction of FMN (ox, sq, or hq) with the corresponding apoprotein (horizontal equilibria on the right) are denoted ΔG_i. [PROTEIN$^{(ox)}$, the mixture of structures found in X-ray analysis of wild type, interacts with FMNox, etc.] The ΔG_i values are not the same as the measured binding free energies, which are for reaction of FMN with apoprotein. The measured shifts in potential, ΔE, relative to that of free FMN, in the right-hand vertical limbs, equal the sum of the steps in each box; e.g. $\Delta E(ox/sq) = \Delta G_c^{ox/sq} + \Delta G_i^{sq} - \Delta G_i^{ox}$. Mutations will impose changes in the free energies of the various steps, denoted $\delta\Delta G$ in the text.

REFERENCES

Alexandrescu, A. T., Ulrich, E. L., & Markley, J. L. (1989) *Biochemistry 28*, 204−211.

Amman, E., Brosious, J., & Ptashne, M. (1983) *Gene 25*, 167−178.

Anderson, A. G., & Hermans, J. (1988) *Proteins: Struct., Funct., and Genet. 3*, 262−265.

Anderson, R. F. (1983) *Biochim. Biophys. Acta 722*, 158−162.

Brünger, A. T. (1992) *X-PLOR, Version* 3.1, Yale University, New Haven, CT.

Brünger, A. T., Krukowski, A., & Erickson, J. (1990) *Acta Crystallogr. A 46*, 585−593.

Bull, C., & Ballou, D. P. (1988) *J. Biol. Chem. 256*, 12673−12680.

Burkhart, B. M., Ramakrishnan, B., Yan, H., Reedstom, R. J., Markley, J. L., Straus, N. A., & Sundaralingam, M. (1995) *Acta Crystallogr. D 51*, 318−330.

Burnett, R. M., Darling, G. D., Kendall, D. S., LeQuesne, M. E., Mayhew, S. G., Smith, W. W., & Ludwig, M. L. (1974) *J. Biol. Chem. 249*, 4383−4392.

Caldeira, J., Palma, P. N., Regalla, M., Lampreia, J., Calvete, J., Schafer, W., LeGall, J., Moura, I., & Moura, J. J. (1994) *Eur. J. Biochem. 220*, 987−995.

Cambillau, C., & Horjales, E. (1987) *J. Mol. Graphics 5*, 174−177.

Cheng, H. N., & Bovey, F. A. (1977) *Biopolymers 16*, 1465−1472.

Clark, W. M. (1972) *Oxidation-Reduction Potentials of Organic Systems*, Robert E. Krieger Publishing Co., Huntington, NY.

Correll, C. C. (1992) Ph.D. Thesis, University of Michigan, Ann Arbor, MI.
Draper, R. D., & Ingraham, L. L. (1968) *Arch. Biochem. Biophys. 125*, 802−808.
Dutton, P. L., & Wilson, D. F. (1974) *Biochim. Biophys. Acta 346*, 165−212.
Eaton, W. A., Hofrichter, J., Makinen, M. W., Andersen, R. D., & Ludwig, M. L. (1975) *Biochemistry 14*, 2146−2151.
Eberhardt, E. S., Loh, S. N., Hinck, A. P., & Raines, R. T. (1992) *J. Am. Chem. Soc. 114*, 5437−5439.
Engh, R. A., & Huber, R. (1991) *Acta Crystallogr. A 47*, 392−400.
Eren, M., & Swenson, R. P. (1989) *J. Biol. Chem. 264*, 14874−14879.
Fox, R. O., Evans, P. A., & Dobson, C. M. (1986) *Nature 320*, 192−194.
Franken, H.-D., Ruterjans, H., & Müller, F. (1984) *Eur. J. Biochem. 138*, 481−489.
Fukuyama, K., Wakabayashi, S., Matsubara, H., & Rogers, L. J. (1992) *J. Mol. Biol. 225*, 775−789.
Hagler, A. T., Osguthorpe, P., Dauber-Osguthorpe, P., & Hempel, J. C. (1985) *Science 227*, 1309−1315.
Hall, L. H., Bowers, M. L., & Durfor, C. N. (1987a) *Biochemistry 26*, 7401−7409.
Hall, L. H., Orchard, B. J., & Tripathy, S. K. (1987b) *Int. J. Quantum Chem. 31*, 217−242.
Hendrickson, W. A. (1985) *Methods Enzymol. 115*, 252−270.
Herzberg, O., & Moult, J. (1991) *Proteins: Struct., Funct., Genet. 11*, 223−229.
Hinck, A. P., Eberhardt, E. S., & Markley, J. L. (1993) *Biochemistry 32*, 11810−11818.
Hoard, L. H., & Nordman, C. E. (1979) *Acta Crystallogr. A 35*, 1010−1015.
Hodel, A., Rice, L. M., Simonson, T., Fox, R. O., & Brünger, A. (1995) *Protein Sci. 4*, 636−654.
Hoover, D. M., Matthews, R. G., & Ludwig, M. L. (1994) in *Flavins and Flavoproteins 1993* (Yagi, K., Ed.) pp 359−362, Walter de Gruyter & Co., Berlin.
Janin, J., Wodak, S., Levitt, M., & Maigret, B. (1978) *J. Mol. Biol. 125*, 357−386.
Jorgensen, W. L., & Gao, J. (1988) *J. Am. Chem. Soc. 110*, 4212−4216.
Kabsch, W., & Sander, C. (1983) *Biopolymers 22*, 2577−2637.
Kazarinova, N. F., Solomko, K. A., & Kotelenets, M. N. (1967) *Chem. Abstr. 67*, 2975d.
Kraulis, P. J. (1991) *J. Appl. Crystallogr. 24*, 946−950.
Kunkel, A. T., Roberts, J. D., & Zakour, R. A. (1987) *Methods Enzymol. 154*, 367−382.
Laudenbach, D. E., Straus, N. A., Pattridge, K. A., & Ludwig, M. L. (1988) in *Flavins and Flavoproteins 1987* (Edmondson, D. E., & McCormick, D. B., Eds.) pp 249−260, Walter de Gruyter & Co., Berlin, New York.
Leenders, R., Kooijman, M., van Hoek, A., Veeger, C., & Visser, A. J. W. G. (1993) *Eur. J. Biochem. 211*, 27−45.
Leenders, R., van Gunsteren, W. F., Berendsen, H. J. C., & Visser, A. J. W. G. (1994) *Biophys. J. 66*, 634−645.
Lewis, P. N., Momany, F. A., & Scheraga, H. A. (1973) *Biochim. Biophys. Acta 303*, 211−229.
Ludwig, M. L., & Luschinsky, C. L. (1992) in *Chemistry and Biochemistry of Flavoenzymes III* (Müller, F., Ed.) pp 427−466, CRC Press, Boca Raton, FL.
Ludwig, M. L., Andersen, R. D., Mayhew, S. G., & Massey, V. (1969) *J. Biol. Chem. 244*, 6047−6048.
Ludwig, M. L., Burnett, R. M., Darling, G. D., Jordan, S. R., Kendall, D. S., & Smith, W. W. (1976) in *Flavins and Flavoproteins* (Singer, T. P., Ed.) pp 393−404, Elsevier Scientific Publishing Co., Amsterdam.
Ludwig, M. L., Schopfer, L. M., Metzger, A. L., Pattridge, K. A., & Massey, V. (1990) *Biochemistry 29*, 10364−10375.
Ludwig, M. L., Pattridge, K. A., Eren, M., & Swenson, R. P. (1991) in *Flavins and Flavoproteins 1990* (Curti, B., Ronchi, S., & Zanetti, G., Eds.) pp 423−428, Walter de Gruyter & Co., Berlin.
Ludwig, M. L., Dixon, M. M., Pattridge, K. A., & Swenson, R. P. (1994) in *Flavins and Flavoproteins 1993* (Yagi, K., Ed.) pp 363−366, Walter de Gruyter & Co., Berlin.
Luschinsky, C. L., Dunham, W. R., Osborne, C., Pattridge, K. A., & Ludwig, M. L. (1991) in *Flavins and Flavoproteins 1990* (Curti, B., Ronchi, S., & Zanetti, G., Eds.) pp 409−413, Walter de Gruyter & Co., Berlin.
Maigret, B., Perahia, D., & Pullman, B. (1970) *J. Theor. Biol. 29*, 275−291.
Maniatis, T., Fritsch, E. F., & Sambrook, J. (1982) *Molecular Cloning: A Laboratory Manual*, Cold Spring Harbor Laboratory Press, Plainview, NY.
Massey, V., & Hemmerich, P. (1978) *Biochemistry 17*, 9−16.
Mayhew, S. G. (1971) *Biochim. Biophys. Acta 235*, 276−288.
Mayhew, S. G. (1977) *Eur. J. Biochem. 85*, 535−547.
Mayhew, S. G., & Massey, V. (1969) *J. Biol. Chem. 244*, 794−802.
Mayhew, S. G., & Ludwig, M. L. (1975) in *The Enzymes* (Boyer, P., Ed.) 3rd ed., Vol. 12, pp 57−117, Academic Press, New York.
Mayhew, S. G., & Tollin, G. (1992) in *Chemistry and Biochemistry of Flavoenzymes III* (Müller, F., Ed.) pp 389−426, CRC Press, Boca Raton, FL.
Mayr, L. M., Willbold, D., Rosch, P., & Schmid, F. X. (1994) *J. Mol. Biol. 240*, 288−293.
Milner-White, E. J., & Poet, R. (1986) *Biochem. J. 240*, 289−292.
Peters, D., & Peters, J. (1981) *J. Mol. Biol. 85*, 107−123.
Pettitt, B. M., & Karplus, M. (1985) *Chem. Phys. Lett. 121*, 194−201.
Rao, S. T., Shaffie, F., Yu, C., Satyshur, K. A., Stockman, B. J., Markley, J. L., & Sundaralingam, M. (1992) *Protein Sci. 1*, 1413−1427.
Reid, L. S., & Thornton, J. M. (1989) *Proteins 5*, 170−182.
Richardson, J. S. (1981) *Adv. Protein Chem. 34*, 167−339.
Sanger, F., Nicklen, S., & Coulson, A. R. (1977) *Proc. Natl. Acad. Sci. U.S.A. 74*, 5463−5467.
Schulz, G. E., & Schirmer, R. H. (1979) *Principles of Protein Structure*, Springer-Verlag, New York.
Scully, J., & Hermans, J. (1994) *J. Mol. Biol. 235*, 682−694.
Sibanda, B. L., & Thornton, J. (1985) *Nature 316*, 170−174.
Smith, J. A., & Pease, L. G. (1980) *CRC Crit. Rev. Biochem. 8*, 315−399.
Smith, W. W. (1977) Ph.D. Thesis, University of Michigan, Ann Arbor, MI.
Smith, W. W., Burnett, R. M., Darling, G. D., & Ludwig, M. L. (1977) *J. Mol. Biol. 117*, 195−225.
Smith, W. W., Pattridge, K. A., Ludwig, M. L., Petsko, G. A., Tsernoglou, D., Tanka, M., & Yasanobu, K. T. (1983) *J. Mol. Biol. 165*, 737−753.
Stockman, B. J., Krezel, A. M., & Markley, J. L. (1990) *Biochemistry 29*, 9600−9609.
Stockman, B. J., Richardson, T. E., & Swenson, R. P. (1994) *Biochemistry 33*, 15298−15308.
Swenson, R. P., & Krey, G. D. (1994) *Biochemistry 33*, 8505−8514.
Taylor, R., & Kennard, O. (1984) *Acc. Chem. Res. 17*, 320−326.
van Mierlo, C. P. M., Lijnzaad, P., Veervoort, J., Müller, F., Berendsen, H. J. C., & de Vlieg, J. (1990) *Eur. J. Biochem. 194*, 185−198.
Venkatachalam, C. M. (1968) *Biopolymers 6*, 1425−1436.
Watenpaugh, K. D., Sieker, L. C., & Jensen, L. H. (1976) in *Flavins and Flavoproteins, 1976* (Singer, T. P., Ed.) pp 405−410, Elsevier Scientific Publishing Co., Amsterdam.
Watt, W., Tulinsky, A., Swenson, R. P., & Watenpaugh, K. D. (1991) *J. Mol. Biol. 218*, 195−208.
Weiner, S. J., Kollman, P. A., Case, D. A., Singh, U. C., Ghio, C., Alagona, G., Profeta, S., Jr., & Weiner, P. (1984) *J. Am. Chem. Soc. 106*, 765−784.
Whitby, L. G. (1953) *Biochem. J. 54*, 437−442.
Wilmot, C. M., & Thornton, J. M. (1988) *J. Mol. Biol. 203*, 221−232.
Yang, A.-S., Hitz, B., & Honig, B. (1996) *J. Mol. Biol. 259*, 873−882.
Zhou, Z., & Swenson, R. P. (1995) *Biochemistry 34*, 3183−3192.
Zhou, Z., & Swenson, R. P. (1996) *Biochemistry 35*, 15980−15988.

BI962180O